공학박사 학위논문

Performance Enhancement Strategies for Cellular Communication in Unlicensed Spectrum

비면허대역 셀룰라 통신을 위한 성능 향상 기법

2021년 8월

서울대학교 대학원

전기·정보공학부

김 지 훈

Performance Enhancement Strategies for Cellular Communication in Unlicensed Spectrum

지도 교수 박 세 웅

이 논문을 공학박사 학위논문으로 제출함

2021년 7월

서울대학교 대학원

전기·정보공학부

김 지 훈

김지훈의 공학박사 학위 논문을 인준함

2021년 6월

위 원 장: 김 성 철

부위원장: 박 세 웅

위 원: 최 완

위 원: 이 경 한

위 원: 주 창 희

Abstract

The 3rd generation partnership project (3GPP) has standardized long-term evolution (LTE) licensed-assisted access (LTE-LAA) that uses a wide unlicensed band as an alternative solution to the insufficient bandwidth problem of the existing LTE. 3GPP cellular communications in unlicensed spectrum allow transmission only after completing listen-before-talk (LBT) operation. For downlink, the LBT operation helps cellular traffic to coexist well with Wi-Fi traffic. However, cellular uplink transmission is attempted only at the time specifically determined by the base station after having a successful LBT and the user equipment (UE) may suffer transmission failure and delayed transmission due to Wi-Fi interference. As a result, cellular uplink traffic does not coexist well with Wi-Fi traffic. NR-U suffers from the collision issue because its channel access mechanism is similar to that of Wi-Fi. Wi-Fi solves the collision problem through the request-to-send/clear-to-send (RTS/CTS) mechanism. However, NR-U has no way of solving the collision problem. As a result, NR-U suffers severe performance degradation due to collisions as the number of contending nodes increases.

In this dissertation, we consider the following two enhancements to cellular communication in the unlicensed spectrum: (i) Uplink channel access enhancement for solving poor uplink performance and (ii) collision minimization for efficient channel utilization.

First, we mathematically analyze the problem of unfairness between cellular and Wi-Fi for uplink channel access. To address the coexistence problem in unlicensed spectrum, we propose a standard-compliant approach, termed UpChance, which allows the UE to use a minimum length of uplink reservation signal (RS) and the base station to determine the optimal timing for the UE's uplink transmission. Through ns-3 simulation, we verify that UpChance improves the performance of fairness and random

access completion time by up to 88% and 99%, respectively.

Second, we propose to extend an RS duration and use a split RS for reservation in NR-U that consists of front RS and rear RS and design a new collision minimization scheme, termed *R-SplitC*, that contains two components: new split RS operation and contention window size (CWS) control. New split RS operation helps to minimize collisions in NR-U transmissions, and CWS control works to protect the performance of other communication technologies such as Wi-Fi. We mathematically analyze and evaluate the performance of our scheme and confirm that *R-SplitC* improves network throughput by up to 100.6% compared to the baseline RS scheme without degrading Wi-Fi performance.

In summary, we propose standard-compliant uplink channel access enhancement scheme and collision minimization scheme for cellular communication in unlicensed spectrum. Through this research, we achieve enhancements of network performance such as throughput and fairness.

keywords: eLAA, LTE-LAA, MulteFire, NR-U, uplink, unlicensed spectrum, collision, and reservation signal.

student number: 2014-21603

Contents

List of Tables

List of Figures

Chapter 1

Introduction

1.1 Motivation

Using only licensed spectrum with limited bandwidth makes it difficult to meet the recent surge in mobile data demand. Unlicensed spectrum, on the other hand, can use a wide bandwidth. With the new acceptance of the 6 GHz band, the bandwidth of the unlicensed spectrum is much broader. Therefore, cellular communication technologies using a wide range of unlicensed spectrum have been proposed by various organizations. 3GPP proposes LTE-LAA and NR-U, LTE-U forum proposes LTE-U, and MulteFire Alliance proposes MultiFire.

These cellular communications in the unlicensed spectrum have evolved considering the coexistence performance with Wi-Fi previously widely used. Unlike Wi-Fi developed as a completely decentralized system, cellular communication operating in the unlicensed spectrum is developed based on cellular communication operating in the licensed spectrum, so some problems that do not occur in Wi-Fi arise.

First, the uplink transmission requires scheduling from the base station and can only begin at a specific point in time. This behavior prevents fair competition in a coexistent environment with Wi-Fi. Second, in an environment where many base stations transmit, the limitation of listen-before talk (LBT) behavior results in numerous colli-

sions. These collisions result in significant losses in terms of the network because they cause no one to succeed in transmission over a long period.

In this dissertation, we address these two problems. We solve these problems by clearly expressing the problem situation mathematically and proposing standard-compliant solutions. Then, we verify the performance of the solutions through mathematical analysis.

1.2 Main Contributions

1.2.1 Uplink Channel Access Enhancement for Cellular Communication in Unlicensed Spectrum

We propose a standard-compliant approach, termed UpChance, which allows the UE to use a minimum length of uplink reservation signal and the base station to determine the optimal timing for the UE's uplink transmission.

The main contributions of work are three-fold:

- We mathematically analyze the problem of unfairness between Wi-Fi and uplink cellular in unlicensed spectrum because legacy UL cellular access in the unlicensed spectrum does not compete fairly with Wi-Fi traffic.
- To address the unfairness problem, we propose a standard-compliant solution, UpChance, that aims to minimize the usage of UL reservation signal (UL-RS). It includes UE operation for sending a UL-RS and eNB operation for scheduling UL transmission optimally.
- Through ns-3 simulation, we evaluate the performance of UpChance in the presence of cellular and Wi-Fi traffic in terms of fairness and random access delay.

1.2.2 R-SplitC: Collision Minimization for Cellular Communication in Unlicensed Spectrum

We first propose a collision reduction scheme, termed *R-Split*, that minimizes the collision probability in NR-U transmissions by extending RS duration and splitting a legacy dummy RS into two short signals: front RS and rear RS. It places an idle gap of short inter-frame space (SIFS) duration between front RS and rear RS to allow the transmitting gNB to sense the channel. Only the gNB that senses the channel idle during this gap can transmit its rear RS and following data frames. Each gNB randomly selects the position of the idle gap.

R-Split reduces collisions, thereby reducing the contention window size (CWS) of each gNB. The reduced CWS of each gNB may harm Wi-Fi performance compared to the baseline scheme that uses the legacy RS. To avoid this problem, we add a CWS control procedure to *R-Split* to increase the CWS of each gNB and name it as *R-SplitC*.

The main contributions of this work are three-fold:

- We propose *R-Split* that minimizes collisions by extending RS duration and splitting a legacy RS into two short signals. *R-Split* puts a randomly selected SIFS idle gap between two short signals for a RS transmission, which helps gNBs reduce collisions.

- We improve *R-Split* to *R-SplitC* by adding a CWS control procedure that protects Wi-Fi traffic by increasing the CWS of each gNB, which has been reduced by *R-Split*.

- We mathematically analyze *R-Split* and *R-SplitC* in an NR-U only environment and validate our modeling through simulation. We confirm that *R-SplitC* improves the throughput of NR-U significantly compared to the baseline scheme without adversely affecting Wi-Fi performance.

1.3 Organization of the Dissertation

The rest of the dissertation is organized as follows.

Chapter 2 presents a standard-compliant approach, termed UpChance, which allows the UE to use a minimum length of uplink reservation signal and the base station to determine the optimal timing for the UE's uplink transmission.

In Chapter 3, we present a collision reduction scheme, termed *R-Split*, that minimizes the collision probability in NR-U transmissions by extending RS duration and splitting a legacy dummy RS into two short signals. We add a CWS control procedure to *R-Split* to increase the CWS of each gNB and name it as *R-SplitC*.

Finally, Chapter 4 concludes the dissertation with the summary of contributions and discussion on the future work.

Chapter 2

Uplink Channel Access Enhancement for Cellular Communication in Unlicensed Spectrum

2.1 Introduction

Due to the high price and scarce bandwidth of licensed spectrum, cellular communication technologies have been developed to operate in unlicensed and licensed spectrum. The 3rd Generation Partnership Project (3GPP) has standardized long term evolution (LTE) based technologies such as LTE licensed-assisted access (LTE-LAA), enhanced LAA (eLAA), and further enhanced LAA (FeLAA) since 3GPP Release 13 [1–3]. LAA technologies use carrier aggregation (CA) to exploit licensed spectrum as an anchor carrier for control and data communication, while using unlicensed spectrum for data communication only. LTE-LAA makes cellular communication technologies in licensed spectrum such as device-to-device (D2D) offload their traffic to unlicensed spectrum [4].

MulteFire Alliance is in the process of standardizing a stand-alone technology that operates in unlicensed spectrum only [5]. Efforts to use cellular communications in unlicensed spectrum are not limited to LTE, but continued in 5G new radio (NR). The 3GPP has standardized NR in unlicensed spectrum (NR-U) since 3GPP Release 16 [6].

NR-U is considered for both LAA-based operation and stand-alone operation, and is being developed to operate in the sub 7 GHz and mmWave spectrum.

Cellular communications in unlicensed spectrum developed based on LTE-LAA technology use listen-before-talk (LBT) for channel access. LBT helps to determine whether the channel has been idle for a certain period before data transmission, which works similarly to carrier sense multiple access with collision avoidance (CSMA/CA) in Wi-Fi. In the case of downlink (DL) transmission, after the evolved Node B (eNB) successfully performs LBT, it transmits a DL reservation signal (DL-RS) to occupy the channel until the next slot/subframe boundary. The RS is a dummy signal to inform other communication devices that the channel is busy. It helps the eNB to start successful DL transmission when LBT is over.

Uplink (UL) transmission requires more procedures. The user equipment (UE) transmits a scheduling request (SR) to the eNB at a predetermined time. After the eNB receives the SR, it sends the UE a UL grant which carries uplink scheduling information. The UE is allowed to transmit the scheduled UL data only after a successful LBT. Due to its transmission at the predetermined time, the UE may not compete fairly against Wi-Fi devices. This means the channel may not be idle at the scheduled time the UE transmits.

The main contributions of this section are three-fold:

- We mathematically analyze the problem of unfairness between Wi-Fi and uplink cellular in unlicensed spectrum because legacy UL cellular access in the unlicensed spectrum does not compete fairly with Wi-Fi traffic.

- To address the unfairness problem, we propose a standard-compliant solution, UpChance, that aims to minimize the usage of UL reservation signal (UL-RS). It includes UE operation for sending a UL-RS and eNB operation for scheduling UL transmission optimally.

- Through ns-3 simulation, we evaluate the performance of UpChance in the pres-

ence of cellular and Wi-Fi traffic in terms of fairness and random access delay.

2.2 Related Work and Preliminaries

2.2.1 Related Work

Much research is underway to improve the performance of cellular communications in the unlicensed spectrum. In particular, an important issue is the coexistence problem with other communication devices such as Wi-Fi. In [7, 8], the authors improve coexistence performance by modifying the LBT operation. However, these papers focus only on the DL performance of LTE. In [9, 10], the authors propose symmetric energy detection (ED) threshold or common preamble between Wi-Fi and unlicensed cellular for coexistence. Our work can achieve greater performance with these approaches in the asymmetric hidden scenario.

In [11–15], the authors improve coexistence performance by using Wi-Fi characteristics. These works apply part of Wi-Fi technology to LTE in the unlicensed spectrum for coexistence. Such modifications are undesirable for manufacturing real devices due to cost and scalability issues. We propose an approach to improve coexistence performance in a way that is not limited to any specific technology.

In [16–20], the authors focus on UL performance of LTE in the unlicensed spectrum. In [16], the authors propose efficient UL grant transmission. In [17], the authors avoid wasting resources due to hidden terminals through over-scheduling. In [18], the authors propose a scheduling model that takes advantage of the flexible allocation in MulteFire. In [19], the authors mathematically analyze whether eLAA is suitable for coexistence with random access or scheduled access. In [20], the authors propose a dynamic channel selection method using a decentralized deep reinforcement learning approach. Through the channel selection method, eLAA avoids Wi-Fi interference. But they show limited improvement in terms of fairness and access delay. Our work highlights that cellular uplink transmission in unlicensed spectrum has a problem of not

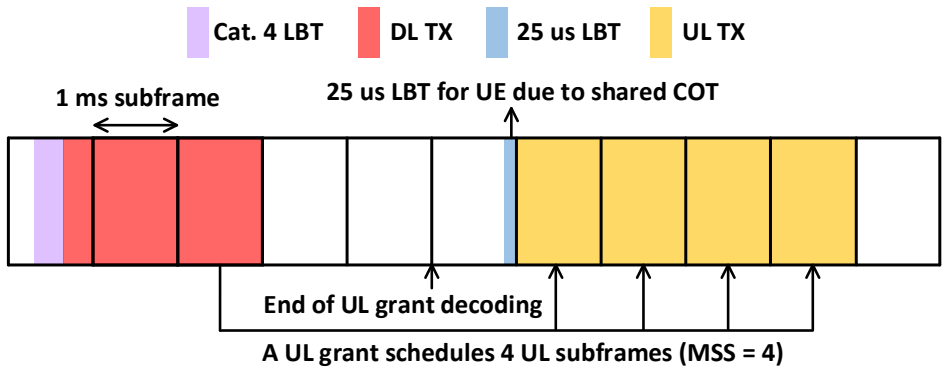

Figure 2.1: eLAA UL data transmission operation (MSS = 4).

properly occupying the channel, especially when the channel is overloaded. To address this problem, we suggest that the UE uses additional Category 4 LBT (Cat. 4 LBT) and UL-RS, and the eNB uses appropriate scheduling considering network traffic.

2.2.2 Preliminaries

LTE-LAA is first proposed in 3GPP Release 13 [1]. It exploits CA to use licensed and unlicensed spectrum at the same time, and uses unlicensed spectrum as an auxiliary carrier. LTE-LAA uses the unlicensed spectrum only for downlink. eLAA and FeLAA are the technologies proposed in 3GPP Release 14 and 15, respectively [2, 3]. eLAA includes uplink operation and FeLAA standardizes uplink partial subframe and autonomous uplink transmission.

In cellular communications in the unlicensed spectrum, there are two types of LBT operation for channel access: 25 μs LBT and Cat. 4 LBT. 25 μs LBT is a simple operation that senses the channel only for 25 μs without backoff operation. If the channel is idle for 25 μs, 25 μs LBT allows transmission. Cat. 4 LBT is a similar operation to CSMA/CA in Wi-Fi. A device waits for a defer period, and if the channel is idle for this period, it starts backoff operation with a backoff counter value randomly selected

within its contention window size (CWS). When the backoff counter reaches zero, the device starts transmission.

For downlink access, the eNB uses 25 μs LBT for special frames such as discovery reference signal, and mostly uses Cat. 4 LBT because of its better coexistence with Wi-Fi compared to 25 μs LBT. After the eNB succeeds in Cat. 4 LBT, it transmits DL-RS until the next slot/subframe boundary and sends DL data.

For uplink access, the eNB chooses the LBT operation type for each UE and informs the UE of this through the UL grant. The eNB shares its channel occupancy time (COT) with the UE (shared COT) within the maximum COT [21]. For instance, if the eNB transmits DL for 4 ms and schedules UL for 4 ms, it may choose 25 μs LBT for the UE to transmit the scheduled UL data.

For the uplink data transmission, the UE should receive a scheduling message through a UL grant. The minimum interval between the UL grant and the scheduled subframe is 4 ms [22], and one UL grant allows transmission of up to four subframes, called multiple-subframe scheduling (MSS) [2]. If the shared COT does not exceed the maximum COT, the UE transmits UL data after a successful 25 μs LBT. If not, the UE should succeed in Cat. 4 LBT first. Fig. 2.1 illustrates an example of eLAA UL operation without Wi-Fi interference.

Random access of cellular communications in the unlicensed spectrum basically uses the same 4-step procedures as in the licensed spectrum. There are four message exchanges for random access [5, 6]. The UE first sends message (msg) 1 called physical random access channel (PRACH) preamble at a PRACH slot if it succeeds in 25 μs LBT before the PRACH slot [5]. The PRACH slot is allotted periodically. The eNB replies to the UE with msg 2 within the random access response (RAR) window. The UE transmits msg 3 at the scheduled time using LBT operation whose type is chosen by the eNB. After receiving msg 3, the eNB transmits msg 4 using Cat. 4 LBT, and the random access operation ends.

2.3 Mathematical Analysis for Unfairness between Uplink Cellular and Wi-Fi

In this section, we mathematically analyze the success probability of 25 μs LBT performed by the UE for uplink transmission.[1] We consider PRACH scenario and UL data scenario.

2.3.1 PRACH scenario

In the PRACH scenario, we consider a coexistence scenario of multiple Wi-Fi transmitters and one UE. All Wi-Fi transmitters have saturated traffic and the UE attempts to transmit a PRACH preamble at the PRACH slot. Fig. 2.2(a) illustrates the PRACH scenario. The UE fails in LBT due to Wi-Fi traffic when it attempts to transmit a PRACH preamble.

We analyze the probability that the UE successfully transmits a PRACH preamble at the PRACH slot based on the Bianchi model [23]. The Bianchi model classifies the channel of each slot into one of three states: successful transmission, collision, and idle. The ratio of each state is $(P_{tr}P_s : P_{tr}(1-P_s) : 1-P_{tr})$. P_{tr} is the probability that at least one Wi-Fi station transmits at a randomly chosen slot and P_s is the probability that only one transmission occurs when the channel is busy.

To get the probability at a certain time, we convert the ratio of each state at a randomly chosen 'slot' to the ratio of each state at a randomly chosen 'time' by multiplying the duration of each state. The ratio of each state at a randomly chosen time is $(T_sP_{tr}P_s : T_cP_{tr}(1-P_s) : \sigma(1-P_{tr}))$. T_s is the average successful transmission duration, T_c is the average collision duration, and σ is the idle slot duration. We define successful transmission probability, collision probability, and idle probability based on the ratio of the states at a randomly chosen time. The successful transmission proba-

[1]The success probability of Cat. 4 LBT performed by the UE is lower than the success probability of 25 μs LBT performed by the UE. It is because 25 μs LBT does not have backoff operation and the defer period of Cat. 4 LBT is longer than 25 μs.

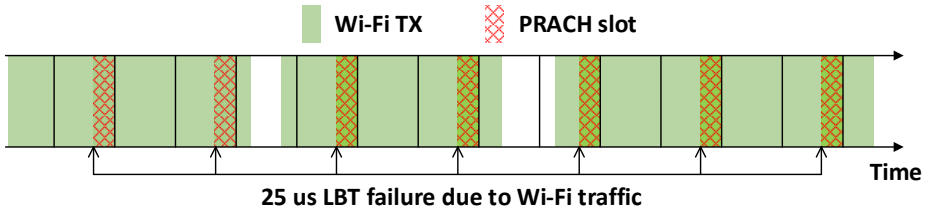

(a) PRACH transmission scenario

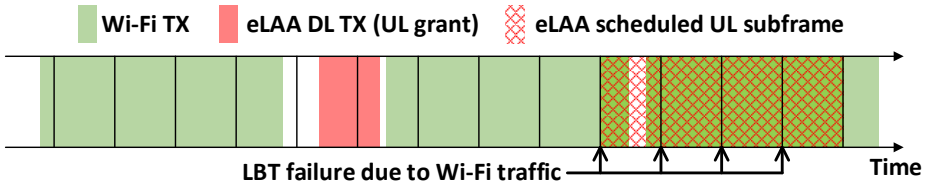

(b) UL data transmission scenario

Figure 2.2: LBT failure scenarios.

bility at a randomly chosen time is defined as

$$P_s^t = \frac{T_s P_{tr} P_s}{T_s P_{tr} P_s + T_c P_{tr}(1-P_s) + \sigma(1-P_{tr})}. \tag{2.1}$$

The collision probability in a randomly chosen time is defined as

$$P_c^t = \frac{T_c P_{tr}(1-P_s)}{T_s P_{tr} P_s + T_c P_{tr}(1-P_s) + \sigma(1-P_{tr})}. \tag{2.2}$$

The idle probability at a randomly chosen time is defined as

$$P_{id}^t = \frac{\sigma(1-P_{tr})}{T_s P_{tr} P_s + T_c P_{tr}(1-P_s) + \sigma(1-P_{tr})}. \tag{2.3}$$

Using these probabilities, we can express the probability that the UE succeeds in 25 μs LBT at a randomly chosen time as

$$P_r = P_s^t \frac{\sigma}{T_s} + P_c^t \frac{\sigma}{T_c} + P_{id}^t. \tag{2.4}$$

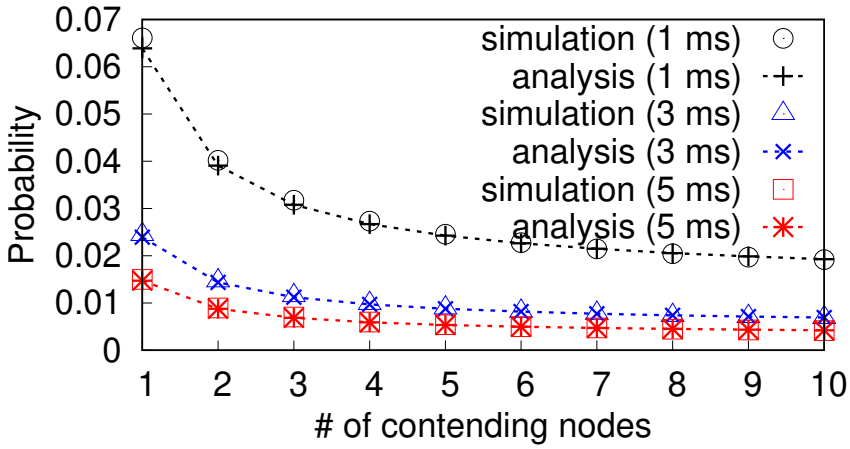

Figure 2.3: Analysis validation in PRACH scenario.

If the channel is in the successful transmission state (P_s^t) or collision state (P_c^t) at a randomly chosen time, 25 μs LBT succeeds only when the chosen time is in the last σ duration of the state. This is because the last part of the successful transmission state and collision state consists of idle distributed coordination function (DCF) inter-frame space (DIFS) duration [23]. If the channel is idle at a randomly chosen time (P_{id}^t), 25 μs LBT always succeeds.[2] The probability that the UE succeeds in 25 μs LBT at the PRACH slot is equal to P_r due to Markov property of the Bianchi model.

To validate our analysis, we implement a coexistence simulator for Wi-Fi and eLAA using MATLAB. Fig. 2.3 shows the probability of the UE's success in 25 μs LBT at the PRACH slot with varying number of contending nodes and Wi-Fi aggregated MAC protocol data unit (A-MPDU) lengths [24]. We observe that the analysis and simulation results become more similar as the number of contending nodes increases, which is consistent with the basic assumptions of the Bianchi model. In most situations, the probability of the UE's success in 25 μs LBT is smaller than 4%. This means that the UE transmits a PRACH preamble with a very low probability under the saturated Wi-Fi traffic condition.

[2]The channel is idle for at least DIFS duration, regardless of the state of the previous slot.

2.3.2 UL data scenario

For UL data transmission, we consider the case where multiple Wi-Fi transmitters and one eNB-UE pair coexist. All Wi-Fi transmitters have saturated traffic and the eNB-UE pair continues to transmit UL grant and UL data. Fig. 2.2(b) illustrates the UL data scenario. The UE attempts to transmit four scheduled UL subframes, but it fails in LBT due to Wi-Fi interference.

We analyze the expected number of successfully transmitted subframes per UL grant based on the Bianchi model [23] and frame-by-frame random walk model [25]. In the frame-by-frame random walk model, a transmission round consists of three periods: random backoff, transmission, and DIFS. In [25], X is a random variable denoting the total time of one transmission round, which is written as

$$X = \sigma * bc_{\text{min}} + T_f + d, \tag{2.5}$$

where bc_{min} is the minimum backoff counter value between two consecutive transmissions, T_f is the frame transmission duration, and d is the DIFS duration.

According to whether the previous transmission is UL grant or Wi-Fi, we define two kinds of bc_{min} distribution: bc^U_{min} and bc^W_{min}. bc^U_{min} is the bc_{min} distribution between the UL grant transmission and the first Wi-Fi transmission after UL grant. When bc^U_{min} is v, the minimum value of the backoff counter values of n Wi-Fi stations is v at the time the UL grant transmission ends. We define bc^U_{min} as

$$\Pr\left(bc^U_{\text{min}} = v\right) = \left(\sum_{l=v}^{CW_{\text{max}}} g_l\right)^n - \left(\sum_{l=v+1}^{CW_{\text{max}}} g_l\right)^n, \tag{2.6}$$

where n is the number of contending Wi-Fi stations, CW_{max} is the Wi-Fi's maximum contention window, and g_l is the probability that a Wi-Fi station has a backoff counter value l when the other nodes end transmissions. g_l equals the conditional probability

that the backoff counter value is $l+1$ under the non-zero backoff counter value.[3] We define g_l as

$$g_l = \frac{\sum_{i=0}^{m} b_{i,l+1}}{1 - \sum_{i=0}^{m} b_{i,0}}, \tag{2.7}$$

where $b_{i,k}$ is the stationary distribution that a Wi-Fi station has the backoff stage i and the backoff counter value k, and m is the maximum backoff stage in the Bianchi model.

bc_{min}^{W} is the bc_{min} distribution between Wi-Fi transmissions. Considering the case of successful transmission and collision, we define bc_{min}^{W} as

$$\begin{aligned} \Pr\left(bc_{\text{min}}^{W} = v\right) =& P_s \left(S_v \times B_v^{n-1} - S_{v+1} \times B_{v+1}^{n-1}\right) \\ &+ \sum_{i=2}^{n} \frac{P_i}{P_{tr}} \left(C_v^i \times B_v^{n-i} - C_{v+1}^i \times B_{v+1}^{n-i}\right), \end{aligned} \tag{2.8}$$

where P_i is the probability that i Wi-Fi stations simultaneously transmit at a slot. S_v, B_v, and C_v are the sum of backoff counter value distribution from v to CW_{max} of a Wi-Fi station that is in the state of successful transmission, idle, and collision, respectively. We express P_i as

$$P_i = \binom{n}{i} \tau^i (1-\tau)^{n-i}, \tag{2.9}$$

where τ is the probability that a Wi-Fi station transmits in a randomly chosen slot [23]. We define S_v as

$$S_v = \sum_{l=v}^{CW_{\text{max}}} h_l, \tag{2.10}$$

[3]The backoff counter values of the Wi-Fi stations decrease by one during UL grant transmission and they are bigger than zero before UL grant transmission. If not, UL grant transmission collides with Wi-Fi due to simultaneous transmission.

where h_l is the probability that a Wi-Fi station has a backoff counter value l right after its successful transmission. We define h_l as

$$h_l = \begin{cases} \frac{1}{CW_{\text{min}}+1}, & 0 \leq l \leq CW_{\text{min}}, \\ 0, & l > CW_{\text{min}}, \end{cases} \tag{2.11}$$

where CW_{min} is the Wi-Fi's minimum contention window. h_l follows a discrete uniform distribution between 0 and CW_{min}. We define B_v as

$$B_v = \sum_{l=v}^{CW_{\text{max}}} g_l, \tag{2.12}$$

and C_v as

$$C_v = \sum_{l=v}^{CW_{\text{max}}} w_l, \tag{2.13}$$

where w_l is the probability that a Wi-Fi station has a backoff counter value l after experiencing a collision. When a Wi-Fi station whose backoff stage is i encounters a collision, the next contention window size becomes $2^{i+1}(CW_{\text{min}} + 1)$. We define w_l as

$$w_l = \frac{\sum_{i=i_s}^{m-1} \left(\frac{b_{i,0}}{2^{i+1}(CW_{\text{min}}+1)} \right) + \frac{b_{m,0}}{CW_{\text{max}}+1}}{\sum_{i=0}^{m} b_{i,0}}, \tag{2.14}$$

where $i_s = \max\left(\lfloor log_2 l \rfloor - log_2(CW_{\text{min}} + 1), 0\right)$.

To succeed in 25 μs LBT for the kth scheduled UL subframe, the kth scheduled UL subframe should be in one of two periods during one transmission round; one is the random backoff period and the other is the last σ period of the DIFS period. We define the probability that the UE succeeds in 25 μs LBT for the kth scheduled UL

subframe as

$$q_k = \sum_{r=1}^{r_{\max}} \Pr\left(d + \sum_{j=1}^{r-1} x_j \leq D_k \leq \sum_{j=1}^{r} x_j - T_f \right) + \sum_{r=1}^{r_{\max}} \Pr\left(d + \sum_{j=1}^{r} x_j - \sigma \leq D_k \leq d + \sum_{j=1}^{r} x_j \right), \tag{2.15}$$

where D_k is the duration between the end of DL transmission of the eNB and the kth scheduled UL subframe, and $r_{\max}$ is the upper bound of the number of transmission rounds where $r_{\max} = \lceil D_k/(d+T_f) \rceil$. The first term on the right hand side indicates the probability that D_k is in the random backoff period of the rth transmission round. The second term represents the probability that D_k is in the last σ period of the DIFS period of the rth transmission round. x_1 follows $bc_{\min}^{U}$ distribution because the first transmission round follows immediately after UL grant transmission. x_j $(j \geq 2)$ follows $bc_{\min}^{W}$ distribution because the jth transmission round comes after Wi-Fi transmission.

We define the probability that the UE succeeds in transmission at the first scheduled UL subframe as

$$p_1 = q_1. \tag{2.16}$$

The UE succeeds in transmission at the first scheduled UL subframe only when the UE succeeds in 25 μs LBT. We also define the probability that the UE succeeds in transmission at the kth scheduled UL subframe as

$$p_k = p_{k-1} + (1 - p_{k-1}) \times q_k, \tag{2.17}$$

where k ranges from 2 to MSS. p_k increases as k increases. This is because if the transmission succeeds in the $(k-1)$th scheduled subframe, the transmission also succeeds in the kth scheduled subframe. If the UE fails in transmission of the $(k-1)$th

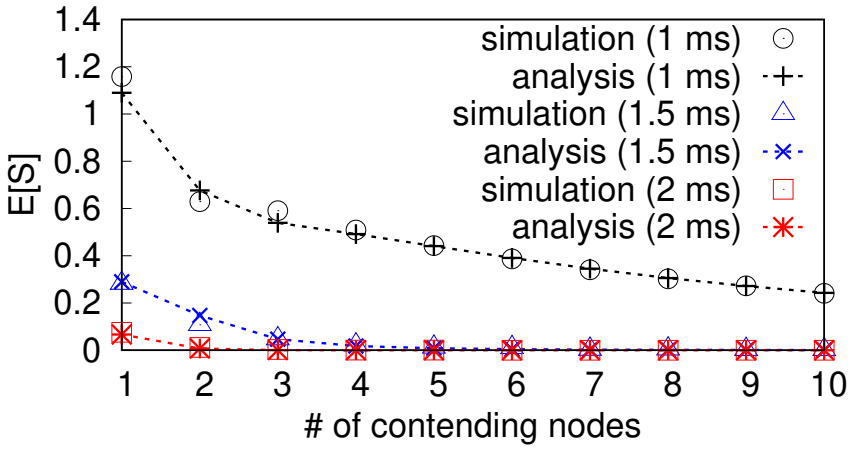

Figure 2.4: Analysis validation in UL data scenario.

scheduled subframe, the UE succeeds in transmission of the kth scheduled UL subframe when it succeeds in 25 μs LBT at the kth scheduled UL subframe. The expected number of successfully transmitted subframes per UL grant is

$$\mathrm{E}\left[S\right] = \sum_{k=1}^{\mathrm{MSS}} p_k. \tag{2.18}$$

We validate the analysis for the UL data scenario using MATLAB simulator. Fig. 2.4 shows $\mathrm{E}\left[S\right]$ with various number of contending nodes and A-MPDU lengths. As in the PRACH scenario, we observe that the analysis and simulation results become closer as the number of contending nodes increases. $\mathrm{E}\left[S\right]$ is close to 0 except when the Wi-Fi A-MPDU length is 1 ms, That is, in the UL data scenario where the UE coexists with Wi-Fi under saturated traffic, UL data transmission is rarely successful.

2.4 Proposed Scheme

In this section, we propose a cellular uplink channel access scheme in the unlicensed spectrum, named UpChance, which is standard-compliant. The UE performs Cat. 4 LBT

first and transmits a minimum length of UL-RS before transmitting data. The eNB schedules UL transmission with optimal delay scheduling, which helps the UE to occupy the channel.

2.4.1 UE Operation

Fig. 2.5(a) shows the overview of UE operation in UpChance. Each UE always measures the most recent N interference lengths to find the maximum interference length (I_{max}). An interference length is the duration of one interference packet.[4] I_{max} is a maximum value among the N measured interference lengths. The UE compares I_{max} with the length of UL-RS (L_{RS}) because I_{max} is the most significant obstacle for the LBT success. I_{max} is an important parameter that shows how fairly the UE occupies the channel.

The UE starts additional Cat. 4 LBT operation after finishing an UL transmission.[5] When the UE succeeds in the additional Cat. 4 LBT, it calculates L_{RS} and compares it with I_{max} to decide whether to transmit UL-RS. L_{RS} is the period from the current time (right after Cat. 4 LBT) to 25 μs before its scheduled UL transmission, varying from time to time. If L_{RS} is shorter than I_{max}, the UE transmits UL-RS to occupy the channel. If not, the UE restarts additional Cat. 4 LBT with the backoff counter value zero until L_{RS} is shorter than I_{max}. After enough time, L_{RS} becomes shorter than I_{max} and the UE transmits UL-RS during L_{RS}.

If an interference packet longer than I_{max} occurs, the UE fails in occupying the channel due to the interference packet. Then, the UE updates I_{max} with the new interference length. This renewal increases the LBT success probability of the UE in the next attempt. The UE minimizes the use of UL-RS to ensure transmission of other devices whenever possible. The UE transmits UL-RS until 25 μs before the scheduled

[4] We consider consecutive interference packets with short inter-frame space (SIFS) idle period one interference packet. It is because SIFS is used for response frame such as acknowledgement frame of Wi-Fi.

[5] This is the same as the post backoff operation of Wi-Fi.

UL transmission. This helps 25 μs LBT to succeed with a very high probability. The failure of 25 μs LBT happens only when interference longer than UL-RS occurs simultaneously with UL-RS transmission. In this case, the UE increases the CWS value of Cat. 4 LBT according to the eLAA specification [2]. Thanks to the 25 μs idle time, UEs within the coverage of the UL-RS increase the success probability of 25 μs LBT for UL data transmission.

2.4.2 eNB Operation

Fig. 2.5(b) shows the overview of eNB operation in UpChance. Before scheduling, the channel saturation detection algorithm determines whether the channel is saturated. If the channel is unsaturated, the eNB schedules UL subframes with a minimum processing delay. If saturated, the eNB expects interfering traffic to come continuously. Considering the UE's decoding time for the scheduling message and LBT failure, the eNB schedules UL transmission with a delay greater than the minimum processing delay, called 'delayed scheduling'.

Each UE decodes the received scheduling message and then accesses the channel for UL transmission using Cat. 4 LBT. Scheduling UL transmission with a larger delay than the minimum processing delay allows the UE to avoid interference and prepare for channel access.[6] If interference occupies the channel during the period that the UE attempts to occupy the channel, the UE cannot occupy the channel. To address this problem, we propose the eNB to use the channel saturation detection algorithm and delayed scheduling algorithm together.

[6]In LTE, the minimum processing delay between UL grant and scheduled UL transmission is 4 ms and the minimum delay between msg 2 and msg 3 in random access is 5 ms [22]. Each UE prepares UL transmission after decoding UL grant or msg 2. The time from the end of scheduling message decoding to UL transmission is about 1 ms [26]. Therefore, each UE has 1 ms to occupy the channel before its scheduled UL transmission.

CHANNEL SATURATION DETECTION

After measuring inter-packet intervals, the eNB determines whether the channel is saturated or not. Transmission of some consecutive packets is considered a 'packet burst' if inter-packet intervals are in the range of [DIFS, AIFS+15$\times\sigma$],[7] where AIFS stands for arbitration inter-frame space. This range includes most inter-packet transmission intervals when packets are continuously transmitted with LBT operation. When LTE-LAA eNBs coexist under saturated traffic, more than 98% of inter-packet transmission intervals fall into this range [27].

If an eNB transmits any packet as part of a packet burst, it considers the channel saturated and predicts that interfering packets will continuously arrive after its transmission. Otherwise, the eNB considers the channel unsaturated. As a delayed scheduling input, the eNB uses the result of packet burst detection including its own transmission.

DELAYED SCHEDULING

If the channel is detected as saturated, the eNB runs delayed scheduling to increase LBT success probability of the UE. The main idea of delayed scheduling is to use the latest interference length information to find the optimal delay for UL scheduling. The basic assumption is that the interference length in the near future (right after the eNB's transmission) is likely to be equal to the recently measured interference length in the saturated channel. In delayed scheduling, the eNB considers all possible cases which occur after its transmission using the recent interference lengths. As a result of delayed scheduling, the eNB gets the optimal delay value (D). D indicates how much longer the interval between a scheduling message and the corresponding scheduled UL subframe is compared to the minimum processing delay. The pseudo-code of delayed scheduling is presented in Algorithm 1.

[7] We do not consider SIFS as an inter-packet interval. If an inter-packet interval is point coordination function inter-frame space (PIFS), we exclude the following packet length from the calculation because it is an intermittent packet such as Wi-Fi beacon.

Algorithm 1 Delayed scheduling algorithm

Input: Interference observation

1: $L = \{L_j | j = 1, \cdots, j_{\text{max}}\}$
2:
3: $R, D \leftarrow 0$
4: **for** d = 0:d_{max} **do**
5: $r_d \leftarrow 0$
6: **for** LT_i = LT_{min}:LT_{max} **do**
7: **for** j = 1:j_{max} **do**
8: $ip \leftarrow \{(LT_i, L_j)\}$
9: $X \leftarrow LT_i + L_j$
10: **if** $X < T_d$ **then**
11: FINDIP(X, d, ip)
12: **else if** $X \geq T_d$ **then**
13: $r_d \leftarrow r_d + \text{Pr}_{d,ip} \cdot S_{d,ip}/C_d$
14: **end if**
15: **end for**
16: **end for**
17: **if** $r_d > R$ **then**
18: $R \leftarrow r_d, D \leftarrow d$
19: **end if**
20: **end for**
21: **return** D

The input of delayed scheduling is a set of measured lengths of interference packets included in the current packet burst (L). The size of L is determined by how many interference packets exist in the current packet burst. The eNB performs an exhaustive search on all delay values (d) (line 4). For each d, the eNB generates all possible interference patterns that can occur between the current DL transmission and the scheduled UL transmission. We define an interference pattern (ip) as a prediction of alternating idle period and busy period over a certain period of time.[8] As a result, an ip consists of one or more (idle period, busy period) combinations, expressed as

$$ip = \{\bigcup_{k=1}^{n} (LT_i, L_j)_k | LT_i \in LT, L_j \in L, n = 1, 2, \cdots\}, \tag{2.19}$$

[8]The idle period occurs due to LBT time of devices and the busy period occurs due to interfere packets.

Algorithm 2 Recursive function for Algorithm 1

1: **function** FINDIP(X, d, ip)
2: **for** LT_i = LT_{min}:LT_{max} **do**
3: **for** j = 1:j_{max} **do**
4: $ip \leftarrow ip \cup \{(LT_i, L_j)\}$
5: $X \leftarrow X + LT_i + L_j$
6: **if** $X < T_d$ **then**
7: FINDIP(X, d, ip)
8: **else if** $X \geq T_d$ **then**
9: $r_d \leftarrow r_d + \text{Pr}_{d,ip} \cdot S_{d,ip}/C_d$
10: **end if**
11: **end for**
12: **end for**
13: **end function**

where LT is a set of LBT times, LT_i is an element of LT, L_j is an element of L, and n denotes the number of (LT_i, L_j) combinations in an ip. Elements of LT are in the range of [DIFS, AIFS+15$\times\sigma$] as in the channel saturation detection algorithm.

To generate an ip, the eNB first selects one (LT_i, L_j) combination in LT and L (lines 6–7). Then, the (LT_i, L_j) combination is the only element of the current ip and sum of LT_i and L_j is the length of the current ip (X) (lines 8–9). If X is larger than the time between the end of DL transmission and the time that the UE finishes decoding of the scheduling message (T_d), an ip is completed (lines 12–13).[9] If not, the eNB selects one more (LT_i, L_j) combination in LT and L and repeats the above procedure using a recursive function (lines 10–11).[10] The pseudo-code of the recursive function is presented in Algorithm 2. In the recursive function, the current ip adds another (LT_i, L_j) combination and updates its length, X (lines 2–5). According to the updated X, the eNB completes an ip or goes through another recursive function (lines 6–9).

After generating an ip, the eNB updates the performance metric r_d for delayed scheduling for a given d (line 13 in Algorithm 1 and line 9 in Algorithm 2). We define

[9]The UE succeeds in Cat. 4 LBT with a high probability after the end of the ip due to its post backoff operation.

[10]If an interference packet transmission ends before the UE decodes a scheduling message, another interference packet follows.

r_d as

$$r_d = \sum_{ip} \mathrm{Pr}_{d,ip} \cdot \frac{S_{d,ip}}{C_d}, \tag{2.20}$$

where $\mathrm{Pr}_{d,ip}$ denotes the probability of the ip, $S_{d,ip}$ denotes the number of UL subframes expected to succeed with the given ip, and C_d denotes the number of subframes required for a period from the scheduling message to the scheduled UL transmission. We can express $\mathrm{Pr}_{d,ip}$ as

$$\mathrm{Pr}_{d,ip} = \prod_{(LT_i, L_j) \in ip} \mathrm{Pr}(LT = LT_i) \cdot \mathrm{Pr}(L = L_j), \tag{2.21}$$

where $\mathrm{Pr}(LT = LT_i)$ denotes the probability that LBT time equals LT_i, and $\mathrm{Pr}(L = L_j)$ denotes the probability that the interference period is L_j.[11] $\mathrm{Pr}_{d,ip}$ decreases as ip has more elements because it multiplies more probability terms. $S_{d,ip}$ varies according to the time the ip ends, i.e., how long X is. For example, if X is a value between T_d and the time between the end of DL and the first scheduled UL subframe (T), $S_{d,ip}$ is the number of scheduled UL data subframes because the UE will transmits all scheduled UL subframes with a high probability. As X increases, $S_{d,ip}$ decreases because the number of remaining scheduled UL subframes decreases. C_d is the delay between the start of eNB's transmission which includes a scheduling message and the end of the scheduled UL subframes. As d increases, C_d also increases because the eNB schedules UL data transmission to rear subframes.

Fig. 2.6 is an example of ip generation. In this example, the eNB selects the first LBT time and interference combination. Because the period of (LT_1+L_1) is smaller than T_d, the eNB selects the second LBT time and interference combination. Then, the ip period (LT_1+L_1+LT_2+L_2) is larger than T_d, and an ip is generated. The ip ends at the second scheduled UL subframe. Thus, $S_{d,ip}$ is two even though the eNB has scheduled four UL subframes. C_d is the period from the UL grant transmission to the end of the scheduled subframe transmission and $\mathrm{Pr}_{d,ip}$ is the product of the

[11] LT_i has a $bc_{\min}$ distribution in Section 2.3 and L_j has a discrete uniform distribution.

probabilities for each component of the ip.

As $S_{d,ip}/C_d$ increases, the throughput of UL transmission increases because the UE transmits more UL subframes in the same period. r_d is the weighted average of $S_{d,ip}/C_d$ for all ip's. Therefore, the eNB can choose the optimal D to make r_d have the largest value.

2.5 Performance Evaluation

In this section, we evaluate the throughput and airtime fairness performance of UpChance in a coexistence environment of eLAA UL and Wi-Fi traffic. Then we show random access performance of UpChance when eLAA random access coexists with Wi-Fi traffic.[12]

2.5.1 Simulation Environments

For ns-3 simulation, we developed the eLAA module based on existing LTE and Wi-Fi modules [28]. eLAA and Wi-Fi interferes with each other, following the 3GPP urban micro (UMi) path loss model.[13] We implemented file transfer protocol (FTP) traffic model, 2×2 multiple-input multiple-output (MIMO), and LBT. Other detailed simulation parameters are summarized in Table 2.1. Wi-Fi traffic is always for downlink and eLAA continues to perform either UL transmission or random access according to the scenario.

An uplink grant schedules four UL subframes. In random access, msg 1 (PRACH preamble), msg 2 (RAR), msg 3, and msg 4 are transmitted. We consider two-cell and multi-cell topologies. Fig. 2.7(a) depicts the two-cell topology with one Wi-Fi cell and one eLAA cell. The Wi-Fi cell consists of one AP and one STA, and the eLAA cell consists of one eNB and one UE. Fig. 2.7(b) illustrates the multi-cell topology with four Wi-Fi cells and one eLAA cell.

[12] Random access follows the MulteFire specification because it is not defined in eLAA.

[13] In realistic deployment in USA, most LAA deployments are in outdoor environments [29].

Table 2.1: Simulation parameters.

Simulation parameters	Value
Simulation time	10 s
File size	0.25 MB
Bandwidth	20 MHz
Wi-Fi PHY	802.11ac, 2×2 MIMO
maximum Wi-Fi A-MPDU bound	1–5 ms, 1,048,575 bytes
Wi-Fi rate adaptation	Minstrel VHT
AP/eNB transmission power	23 dBm
STA/UE transmission power	18 dBm
Wi-Fi CS/CCA threshold	-82 dBm
Wi-Fi CCA-ED threshold	-62 dBm
LTE CCA-ED threshold	-72 dBm
N	20
$d_{\max}$	10
$LT_{\min}$	34 μs
$LT_{\max}$	178 μs

For performance comparison, we consider three competitive schemes: 1) The baseline scheme is the legacy eLAA, which starts UL transmission only when 25 μs LBT succeeds without using RS, 2) UE only scheme applies only the UE operation of UpChance, and 3) DL-RS scheme allows the eNB to continuously transmit DL-RS after transmitting a UL grant or RAR, which helps the UE to occupy the channel until 25 μs before UL transmission.

2.5.2 UL data transmission

We investigate the coexistence performance of UpChance according to the interference length when the channel is saturated. Fig. 2.8(a) shows throughput of Wi-Fi and eLAA with varying Wi-Fi A-MPDU length in the two-cell topology. Fig. 2.8(b) shows airtime performance of Wi-Fi and eLAA, and Jain's fairness index with varying Wi-Fi A-MPDU length. In Fig. 2.8(b), eLAA data means the airtime of the eLAA signal excluding RS, and eLAA RS means the total airtime of DL-RS and UL-RS. We calculate Jain's fairness index using Wi-Fi airtime and eLAA airtime (eLAA data + eLAA RS),

as

$$J(x_1, x_2, \cdots, x_n) = \frac{(\sum_{i=1}^{n} x_i)^2}{n \sum_{i=1}^{n} x_i^2}. \tag{2.22}$$

In the baseline scheme, Wi-Fi takes up most of the throughput and airtime regardless of the Wi-Fi A-MPDU length. This is because the baseline scheme cannot support the coexistence well under the saturated channel. UE only scheme shows better coexistence performance than the baseline scheme because the UE is able to use UL-RS. DL-RS scheme allows eLAA to better coexist with Wi-Fi compared to the baseline. However, due to the long DL-RS interval between UL grant and UL data transmission and the eLAA RS length, DL-RS scheme shows significantly lower throughput than the other three schemes.

UpChance shows a performance improvement of up to 88% in terms of fairness compared to the baseline scheme. When the Wi-Fi A-MPDU length is 1 ms or 3 ms, the results of UpChance and UE only scheme are the same because the result of delayed scheduling is the same as that of the legacy scheduling. In the other cases, UpChance occupies the channel more often compared to UE only scheme thanks to delayed scheduling. As a result, UpChance shows better performance than UE only scheme in various environments. The performance improvement increases with the interference length.

We investigate the coexistence performance of UpChance in the multi-cell topology of four Wi-Fi cells and one eLAA cell. Fig. 2.9 shows throughput and airtime performance. Four Wi-Fi cells have four different Wi-Fi A-MPDU lengths of 5 ms, 4 ms, 3 ms, and 2 ms, respectively. The percentage of channel occupancy of each AP is proportional to the A-MPDU length. The baseline scheme rarely allows eLAA to occupy the channel similarly in the two-cell topology due to the limitations of the legacy LBT operation. UE only scheme shows more performance improvement of eLAA compared to the baseline scheme thanks to the use of UL-RS. DL-RS scheme increases eLAA performance and decreases network throughput compared to the baseline scheme. It

wastes lots of time that can be exploited in the other schemes. UpChance shows improved eLAA performance due to the increased LBT success probability of the UE even under various interference lengths.

Fig. 2.10 shows the network throughput gain of UpChance compared to the baseline scheme according to the file size and the number of files per second of Wi-Fi in the two-cell topology under the unsaturated traffic condition. The product of x-axis and y-axis is the Wi-Fi source rate. For low Wi-Fi source rate, the throughput gain is also low due to low Wi-Fi traffic. With the Wi-Fi source rate, Wi-Fi transmission gradually hinders eLAA transmission, which acts as the baseline scheme. The more the hindrance, the greater the gain of UpChance. The throughput gain of UpChance increases by up to 16.95% as the Wi-Fi source rate increases. UpChance improves performance even when the channel is not saturated. When the Wi-Fi source rate becomes large enough, only Wi-Fi traffic is transmitted in the baseline scheme. However, in UpChance, Wi-Fi and eLAA coexist well. As in Fig. 2.8(a), the network throughput in the baseline scheme is slightly higher than that in UpChance.[14]

2.5.3 Random access

We investigate how well random access is performed in the coexistence environment. In the random access scenario, after completing random access, the UE attempts random access again in the next PRACH slot. Fig. 2.11 shows random access completion time according to the Wi-Fi A-MPDU length in the two-cell topology under saturated Wi-Fi traffic. The random access completion time is the time from when the transmission of msg 1 is desired until the transmission of msg 4 is finished. The results of the maximum y-axis expressed are those of not successfully completed random access.

The baseline scheme does not complete random access operation, regardless of the Wi-Fi A-MPDU length. This is because LBT for msg 3 is almost unsuccessful in

[14]In our simulation, the data rate of eLAA is slightly larger than that of Wi-Fi. However, the network throughput in Wi-Fi only environments is larger than that in coexistence environments due to the distributed nature of Wi-Fi.

an environment where Wi-Fi traffic is saturated. UE only scheme shows the random access completion time of 16.83 ms and 20.59 ms when the Wi-Fi A-MPDU length is 1 ms and 3 ms, respectively, which are much smaller than those shown by the baseline scheme. When the Wi-Fi A-MPDU length is 2 ms, 4 ms, and 5 ms, UE only scheme shows smaller performance improvement compared to the baseline scheme.

The probability of additional Cat. 4 LBT success of the UE varies greatly depending on the length of Wi-Fi frame transmitted immediately after msg 2 transmission, resulting in a large performance difference. When the Wi-Fi A-MPDU length is 1 ms and 3 ms, the transmission of Wi-Fi frame is highly likely to end during the period when the UE performs additional Cat. 4 LBT. Thus, the UE tends to occupy the channel during this period. On the other hand, when the Wi-Fi A-MPDU length is 2 ms, 4 ms, and 5 ms, the transmission of Wi-Fi frame is highly likely to continue for a period during which the UE performs additional Cat. 4 LBT. Thus, the UE is not likely to occupy the channel. As described above, the operation of UE only scheme is greatly affected by the interference.

DL-RS scheme shows more reliable performance than UE only scheme according to the Wi-Fi A-MPDU length. The random access completion time in DL-RS scheme gradually increases with the Wi-Fi A-MPDU length. This is because the probability of LBT success for msg 1 decreases with the Wi-Fi A-MPDU length. In addition, msg 3 transmission is guaranteed through DL-RS transmission, so the transmission probability of msg 3 is not affected by the Wi-Fi A-MPDU length.

UpChance shows the best performance in all the cases compared to the other schemes. It reduces random access completion time by up to 99% compared to the baseline. UpChance has a good ability to cope with various Wi-Fi A-MPDU lengths owing to its eNB operation. When the Wi-Fi A-MPDU length is 1 ms and 3 ms, UpChance shows the same performance as UE only scheme. This is because msg 3 is well transmitted even without the help of delayed scheduling at the eNB. When the Wi-Fi A-MPDU length is 2 ms, 4 ms, and 5 ms, UpChance shows significantly

improved random access performance compared to UE only scheme. This is because msg 3 is scheduled by predicting when the Wi-Fi frame ends.

Fig. 2.12 shows random access completion time in the multi-cell topology. Four Wi-Fi APs have the Wi-Fi A-MPDU length of 5 ms, 4 ms, 3 ms, and 2 ms, respectively. The baseline scheme shows very high random access completion time because random access is rarely successful due to difficulties in transmission of msg 1 and msg 3 as in the two-cell topology. UE only scheme shows better performance than the baseline scheme due to the benefit of UL-RS transmission. DL-RS scheme also has the random access completion time similar to that of UE only scheme. By guaranteeing the msg 3 transmission, it shows better performance than the baseline scheme, but worse performance than UpChance because of the poor msg 1 transmission probability. UpChance shows the best performance thanks to the use of UL-RS and delayed scheduling.[15]

Fig. 2.13 shows the random access completion time gain under unsaturated Wi-Fi traffic in the two-cell topology. The performance in UpChance increases with the Wi-Fi source rate. For low Wi-Fi source rate, random access works well even in the baseline scheme, so there is little random access completion time gain. With the Wi-Fi source rate, UpChance shows gradually improved performance compared to the baseline scheme owing to its successful transmission of msg 1 and msg 3. For the saturated channel, the baseline scheme rarely succeeds in random access. As a result, UpChance shows random access completion time gain of nearly 100% over the baseline scheme.

2.6 Summary

In this chapter, we investigated the uplink channel access problem of cellular communication in the unlicensed spectrum through mathematical analysis, and proposed a standard-compliant solution named UpChance. The UE in UpChance uses a minimum length of uplink reservation signal for contention-based channel access, without

[15]The performance gap between UE only scheme and UpChance in the random access scenario is larger than that in UL data scenario. This is because msg 2 schedules only one subframe for msg 3.

harming the nature of UL multi-access. The eNB in UpChance detects channel saturation and schedules the UE's uplink transmission with the best delay. Through ns-3 simulation, we evaluated the performance of UpChance in UL data transmission and random access scenarios. We confirmed that UpChance achieves fairness performance improvement of up to 88% in the UL data scenario, and the random access completion time gain of up to 99% in the random access scenario.

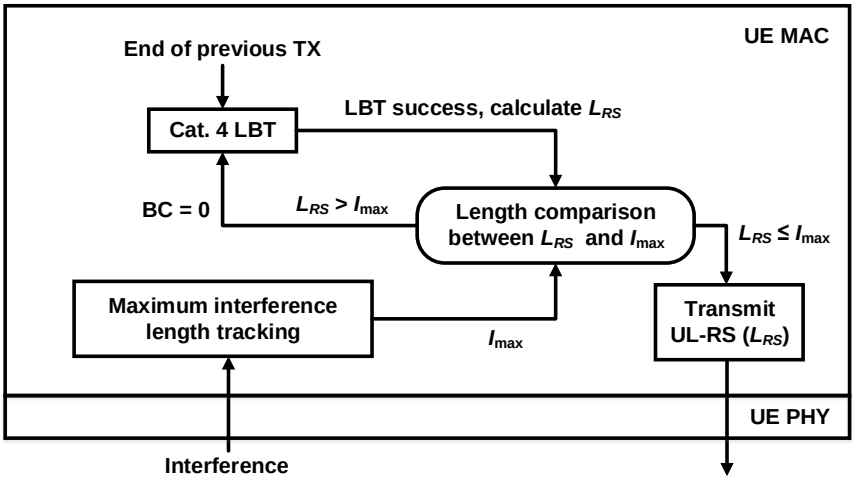

(a) UE operation

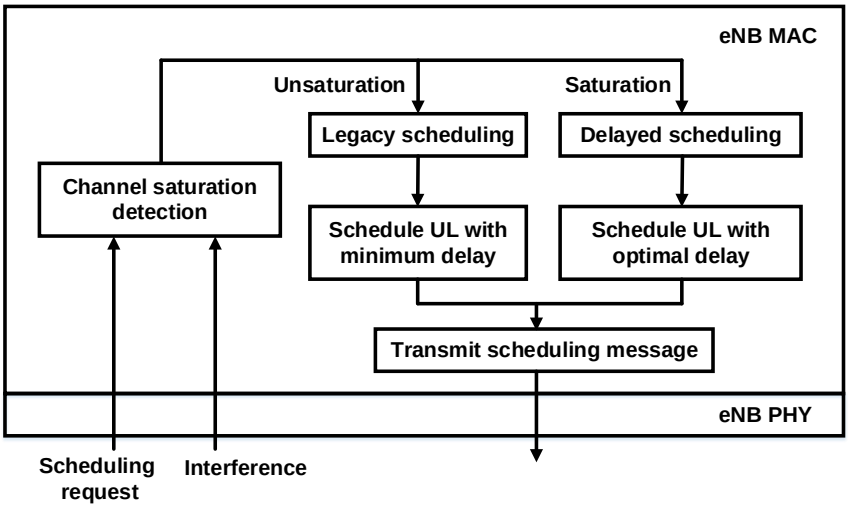

(b) eNB operation

Figure 2.5: UpChance operations.

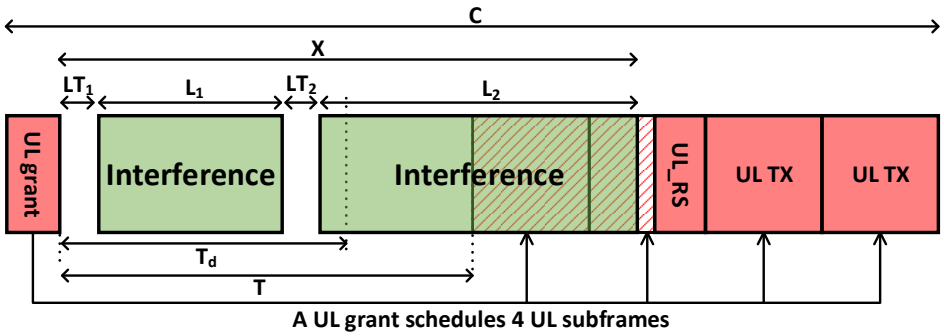

Figure 2.6: An example of interference pattern generation.

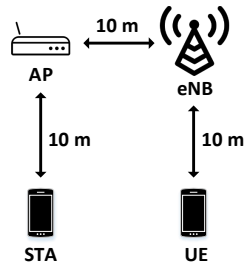

(a) Two-cell topology

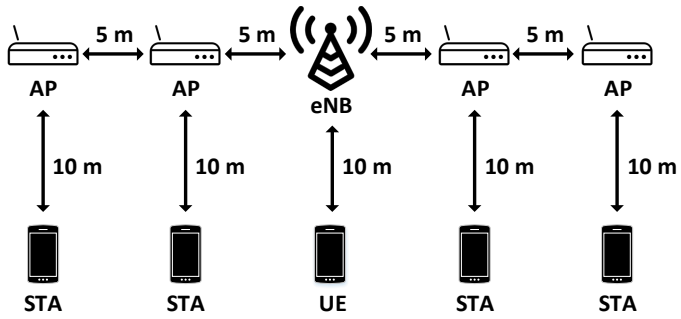

(b) Multi-cell topology

Figure 2.7: Simulation topology.

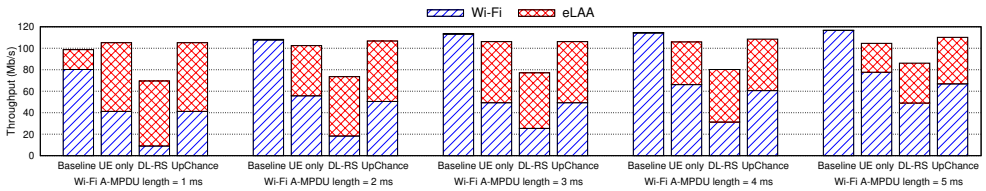

(a) Throughput

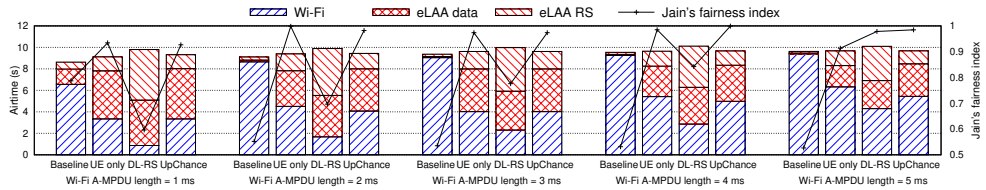

(b) Airtime

Figure 2.8: Performance of UpChance according to the Wi-Fi A-MPDU length in the two-cell topology.

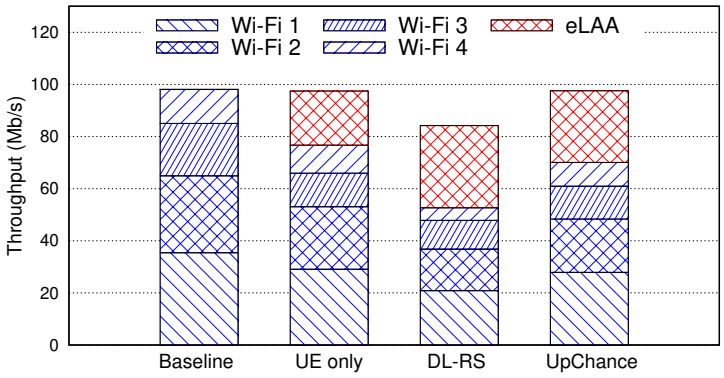

(a) Throughput

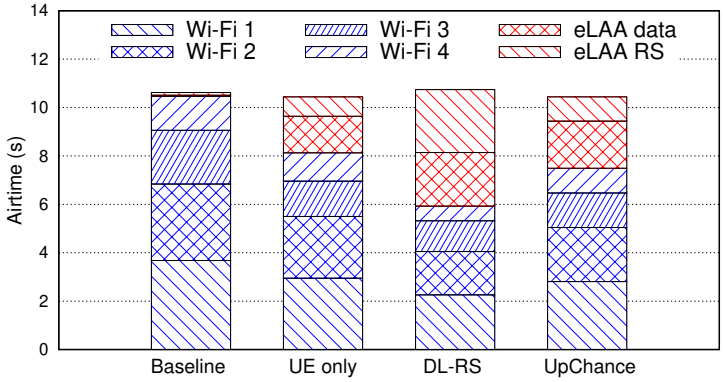

(b) Airtime

Figure 2.9: Performance of UpChance in the multi-cell topology.

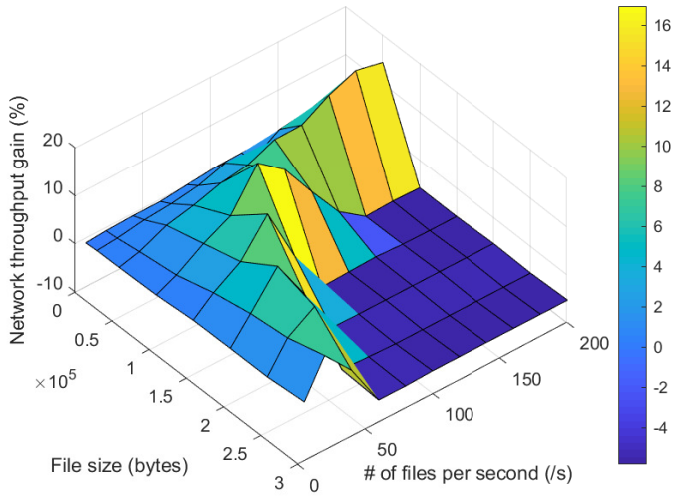

Figure 2.10: Network throughput gain of UpChance in an unsaturated channel environment.

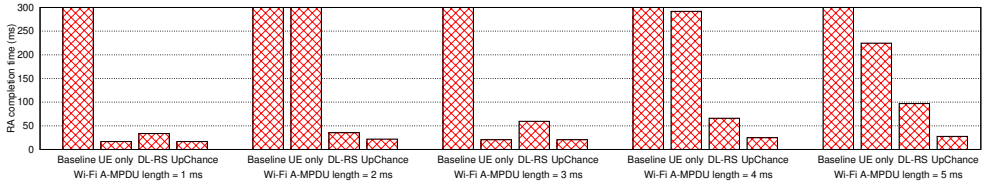

Figure 2.11: Random access performance of UpChance according to the Wi-Fi A-MPDU length.

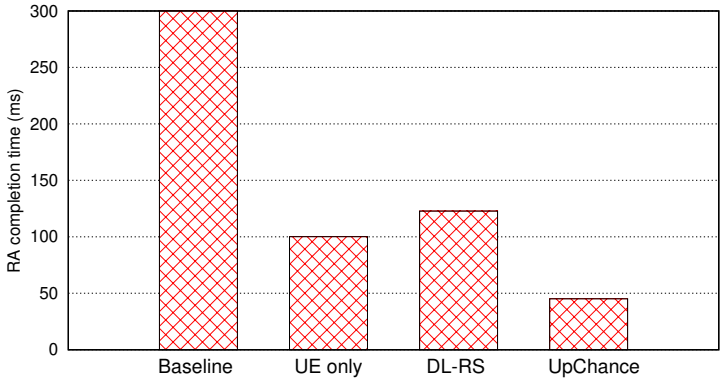

Figure 2.12: Random access performance of UpChance in multi-cell topology.

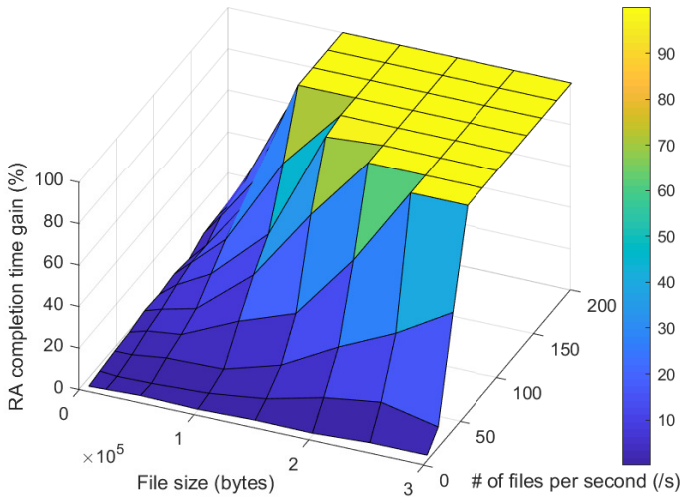

Figure 2.13: Random access completion time gain of UpChance in unsaturated Wi-Fi traffic.

Chapter 3

R-SplitC: Collision Minimization for Cellular Communication in Unlicensed Spectrum

3.1 Introduction

As mobile data demand has increased rapidly in recent years, all demands cannot be satisfied with the limited licensed band. The 3rd generation partnership project (3GPP) first standardized long-term evolution (LTE) licensed-assisted access (LTE-LAA) in 3GPP Release 13 by developing LTE that uses only the existing licensed band to share unlicensed bands [1]. The standardization of enhanced LAA (eLAA) in 3GPP Release 14 and further enhanced LAA (feLAA) in 3GPP Release 15 has been continued [2, 3]. The standardization of the new radio (NR) in unlicensed band (NR-U), which is an NR operating in the unlicensed band, is underway, a key technology for 5G [6,30]. Research on cellular communication operating in the unlicensed band is active recently, and the actual deployment is gradually progressing. In Chicago, cellular operators such as AT&T, Verizon, and T-Mobile have installed numerous LTE-LAA eNBs [29].

Cellular communication technologies in unlicensed spectrum proposed by 3GPP operate in a distributed manner. That is, each device goes through a channel sensing

process, and only when the channel is idle, it can start transmission. This operation suffers the collision problem due to simultaneous transmissions as the number of competing devices increases. Wi-Fi solves the collision problem by sending and receiving short control frames called request-to-send/clear-to-send (RTS/CTS) frames.

However, NR-U shows a different situation. After completing the LBT, an NR-U gNB transmits a dummy signal called reservation signal (RS) until the next mini-slot starting point and starts data transmission. The length of RS lies between 0 and 71 μs, depending on the time the LBT is completed.[1] Because an NR-U gNB starts data transmission only at the orthogonal frequency division multiplexing (OFDM) symbol boundary and its decoding time is longer than that in Wi-Fi, it cannot exchange short frames like RTS/CTS on Wi-Fi in a short time. This means that NR-U has limitations in solving the collision problem.

In this chapter, we first propose a collision reduction scheme, termed *R-Split*, that minimizes the collision probability in NR-U transmissions by extending RS duration and splitting a legacy dummy RS into two short signals: front RS and rear RS. It places an idle gap of short inter-frame space (SIFS) duration between front RS and rear RS to allow the transmitting gNB to sense the channel. Only the gNB that senses the channel idle during this gap can transmit its rear RS and following data frames. Each gNB randomly selects the position of the idle gap.

R-Split reduces collisions, thereby reducing the contention window size (CWS) of each gNB. The reduced CWS of each gNB may harm Wi-Fi performance compared to the baseline scheme that uses the legacy RS. To avoid this problem, we add a CWS control procedure to *R-Split* to increase the CWS of each gNB and name it as *R-SplitC*.

The main contributions of this section are three-fold:

- We propose *R-Split* that minimizes collisions by extending RS duration and splitting a legacy RS into two short signals. *R-Split* puts a randomly selected SIFS idle gap between two short signals for an RS transmission, which helps

[1] This range is for 30 kHz subcarrier spacing.

gNBs reduce collisions.

- We improve *R-Split* to *R-SplitC* by adding a CWS control procedure that protects Wi-Fi traffic by increasing the CWS of each gNB, which has been reduced by *R-Split*.

- We mathematically analyze *R-Split* and *R-SplitC* in an NR-U only environment and validate our modeling through simulation. We confirm that *R-SplitC* improves the throughput of NR-U significantly compared to the baseline scheme without adversely affecting Wi-Fi performance.

3.2 Related Work and Preliminaries

3.2.1 Related Work

There have been many studies on the performance of LTE-LAA and NR-U. In particular, there are many studies on the coexistence performance of LTE-LAA and Wi-Fi. In [7, 8, 31–33], the authors increase the coexistence performance by modifying LBT operation. In [15], the authors adapt the maximum channel occupancy time (MCOT) of LTE-LAA to the aggregated medium access control protocol data unit (A-MPDU) duration of Wi-Fi for fair channel occupancy.

Many LTE-LAA studies mathematically analyze the throughput performance based on Bianchi model [23]. In [27], the authors analyze the LTE-LAA throughput performance considering LTE-LAA frame structure, including the ending partial subframe (EPS). In [34–37], the authors analyze the coexistence performance of LTE-LAA and Wi-Fi. We conduct the performance analysis of our proposed scheme based on [23,27] with the consideration of LTE-LAA frame structure.

Some studies consider the collision problems in LTE-LAA and NR-U. In [38], the authors raise a problem of modulation and coding scheme (MCS) underestimation due to collisions. The authors solve the problem by distinguishing the underestimated

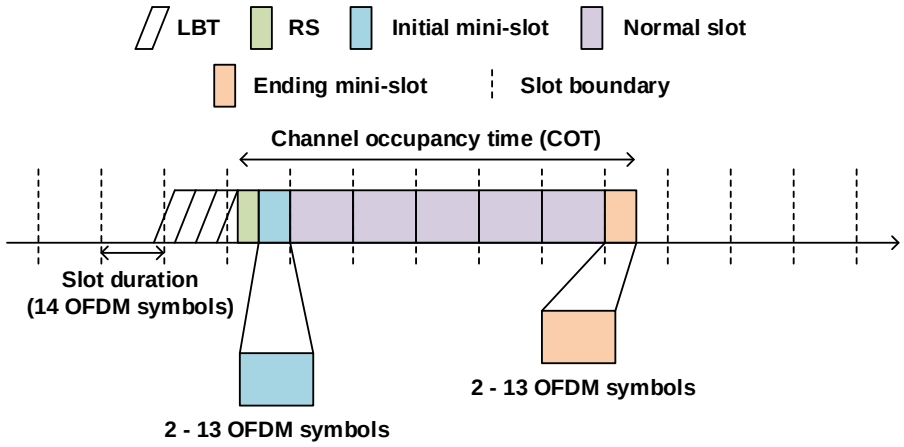

Figure 3.1: NR-U frame structure.

channel quality information (CQI) from normal CQI. However, this work does not decrease collisions. In [39], the authors find that if a collision between LTE-LAA and Wi-Fi which uses RTS/CTS occurs, the fairness problem arises because only LTE-LAA nodes successfully transmit. The authors solve the problem by modifying RS. However, they only consider the coexistence between LTE-LAA and Wi-Fi which uses RTS/CTS. In [40], the authors propose an LBT technique for collision resolution of NR-U. However, RS duration in NR-U is too short for collision resolution. Our work reduces collisions that cause MCS underestimation and solves the collision problem between NR-U nodes by extending RS duration and designing an RS frame structure with various priorities. It does not incur any harmful impact on Wi-Fi traffic regardless of RTS/CTS operation.

3.2.2 NR-U

NR-U is first standardized in 3GPP Release 16 and uses licensed and unlicensed bands together or unlicensed bands only, unlike NR that uses only the licensed band [6]. In the unlicensed band, an NR-U gNB starts transmission only after completing the LBT

operation. It can occupy the channel up to MCOT defined in the specification. In the case of priority class 3, MCOT is 8 ms when other communication technologies exist, and 10 ms otherwise [6].

3.2.3 listen-before-talk (LBT)

An NR-U gNB starts transmission after completing one of the two types of LBT: Category 4 LBT and 25 μs LBT. First, Category 4 LBT is an operation similar to Wi-Fi's CSMA/CA operation. The gNB first senses the channel for a defer period of arbitrary inter-frame space (AIFS) duration. If the channel is idle during the AIFS, the gNB starts backoff operation. The gNB randomly selects a backoff counter value in the range of [0, CW]. If 80% or more of Hybrid ARQ feedback of the starting slot of the previous transmission of the gNB is NACK, the gNB increases the CWS. Otherwise, the gNB resets the CWS to the minimum value. The range of the CWS value depends on the priority class of the transmitted data. In this chapter, we mainly consider best effort traffic that has the CWS range in [16, 32, 64].

Second, 25 μs LBT is an operation enabling transmission without a backoff operation when the channel is idle for 25 μs. Most of transmissions of the gNB use Category 4 LBT and only intermittent transmissions such as discovery reference signals use 25 μs LBT.

3.2.4 reservation signal and mini-slot

Fig. 3.1 shows the NR-U frame structure. When a gNB succeeds in LBT operation, it transmits an RS until the next mini-slot start point. The RS is a dummy signal whose length varies depending on the end time of LBT and informs other devices of the channel occupancy of the gNB. NR-U starts data transmission at OFDM symbol boundaries. If the next OFDM symbol boundary after LBT success is a slot boundary, the gNB transmits a normal slot after the RS. Conversely, if the next OFDM symbol boundary after LBT success is a OFDM symbol boundary (i.e., not a slot boundary),

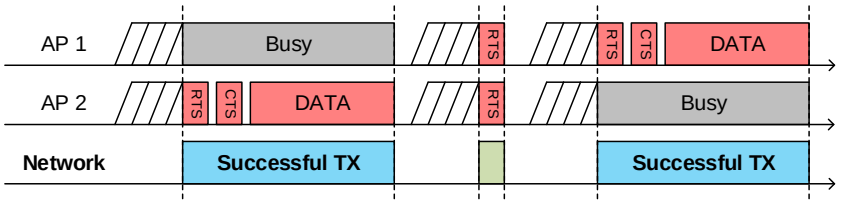

(a) Collision between Wi-Fi with RTS/CTS

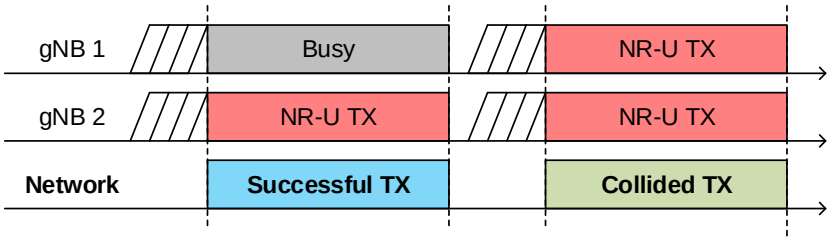

(b) Collision between LTE-LAA

Figure 3.2: Collision cases in the unlicensed band.

the gNB transmits an initial mini-slot (IMS) after the RS. Each initial mini-slot consists of 2–13 OFDM symbols.

To transmit data frames of maximum length not exceeding MCOT, NR-U uses 12 types of ending mini-slot (EMS). Each EMS consists of 2–13 OFDM symbols. In this chapter, we name each of the 13 EMS types as EPS type i ($i = 1, \cdots, 13$), where EMS type 1 is a transmission that does not use EMS. As i increases, EMS type i uses ending mini-slot with i OFDM symbols.

3.2.5 Wi-Fi

Wi-Fi has a channel access mechanism of CSMA/CA. For best effort traffic, the maximum CWS in Wi-Fi is 1024. Wi-Fi uses A-MPDU for a long transmission with its maximum duration of 5.484 ms in IEEE 802.11ac [24]. For RTS/CTS operation, a sender first transmits an RTS frame before data transmission. After decoding the RTS

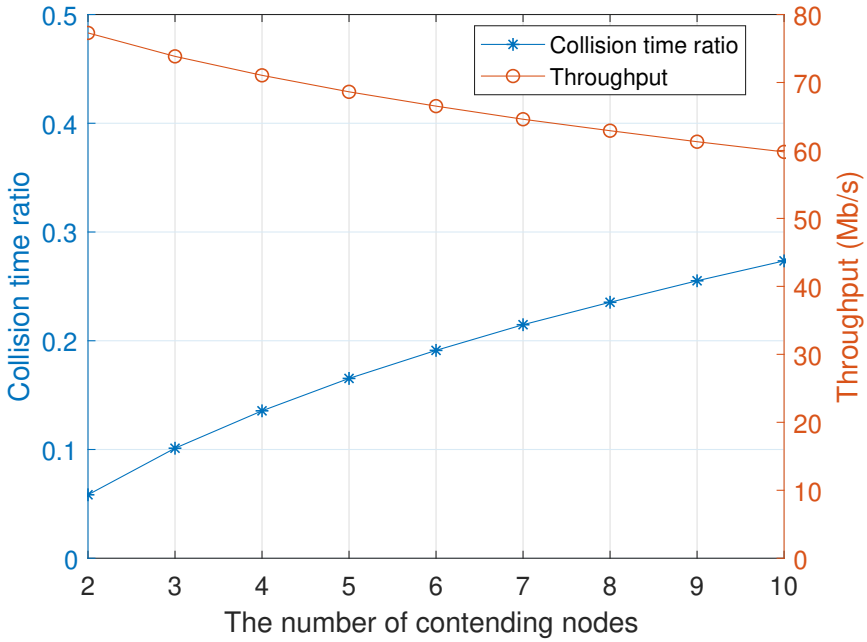

Figure 3.3: Collision time ratio and throughput according to the number of contending nodes.

frame, the receiver transmits a CTS frame to the sender. Then, a data frame is transmitted only when the sender successfully decodes the CTS frame. If the RTS frame collides with other transmissions, the receiver fails to decode the RTS frame and does not send the CTS frame. The sender restarts CSMA/CA operation with increased CWS after CTS timeout.

When the channel is saturated, more collisions occur with the number of contending nodes. In the case of Wi-Fi using RTS/CTS, no CTS response means that a collision has occurred. However, in the case of NR-U, there is no way of detecting collisions during a transmission. NR-U gNBs transmit data as close to the length of MCOT as possible when the traffic is saturated. Therefore, if a collision occurs, all gNBs involved in the collision waste time because no node can successfully transmit during the collision. Figs. 3.2 (a) and (b) show examples of collisions in Wi-Fi and NR-U, respectively. From a network point of view, colliding transmissions cause more

time wasted in NR-U than in Wi-Fi. With the number of collisions, the efficiency in NR-U is significantly worse than that in Wi-Fi.

NR-U has a mechanism to increase CWS to minimize collisions. However, the mechanism cannot completely resolve collisions. Fig. 3.3 shows our simulation results of the collision time ratio and network throughput in an NR-U only network with the number of gNBs.[2] As the number of gNBs increases, the collision time ratio increases, and the network throughput decreases. The results show that the damage caused by collisions increases with the number of contending nodes despite the CWS increase mechanism.

3.3 Proposed Scheme

In this section, we propose *R-Split* that aims to enhance NR-U performance by minimizing collisions. We also propose *R-SplitC* by adding an operation to *R-Split* to protect the transmission of other communication devices such as Wi-Fi. Fig. 3.4 shows the flow chart of *R-SplitC* that consists of two main features: new RS operation and CWS control. *R-Split* uses the new RS operation only without CWS control. The new RS operation consists of two procedures: RS extension and RS split. RS extension extends RS duration until gNB has the desired number of RS types and reduces data parts to maintain COT shorter than MCOT. RS split consists of three procedures: front RS transmission, 16 μs idle gap sensing, and rear RS transmission, where 16 μs is SIFS duration used for collision avoidance. There are a TX/RX turnaround time and a backoff slot in the 16 μs idle gap.[3]

Assume that there are three gNBs transmitting RSs after simultaneous LBT success. Each gNB transmits a front RS with a length randomly chosen within the limited length. Then it performs channel sensing for the idle gap of 16 μs. If gNB 2 has the

[2]The collision time ratio is a ratio of collision time to the total simulation time.

[3]If the TX/RX turnaround time is shorter than 7 μs, 16 μs idle gap is possible for channel sensing. In [41], the TX/RX turnaround time is shorter than 2 μs. If the regulation of the TX/RX turnaround time is shorter than 7 μs, the duration of the idle gap can be shorter than 16 μs.

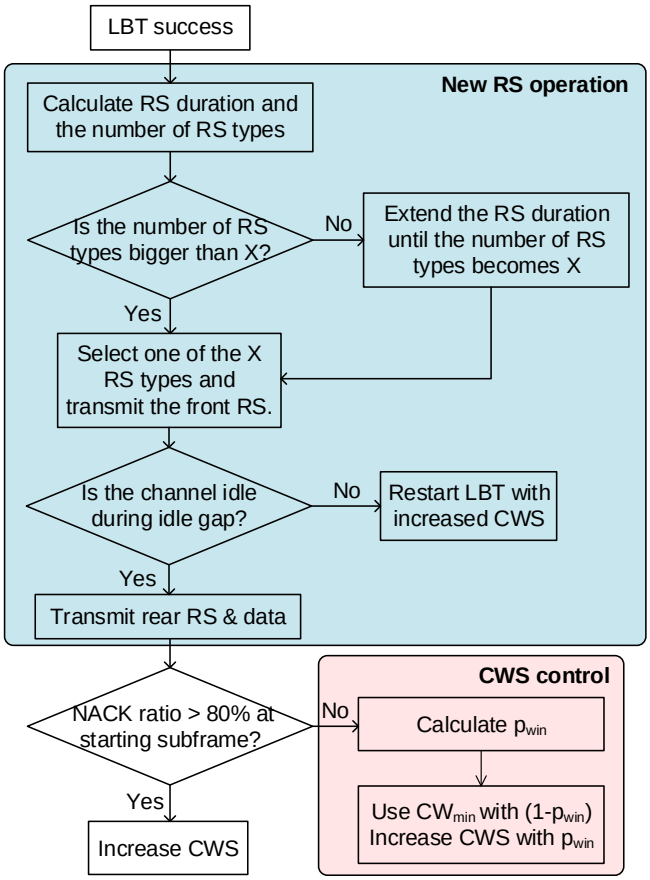

Figure 3.4: Flow chart of *R-SplitC*.

highest priority among the three (i.e., the longest front RS length), gNB 2 detects the channel idle during its idle gap. Then only the gNB 2 is allowed to transmit its rear RS and data slots.[4]

Since each of gNBs 1 and 3 has a shorter front RS length than gNB 2, they sense the channel busy during the idle gap and cannot transmit their rear RS. They restart LBT with increased CWS. The increased transmission success rate of each gNB contributes to lowering its CWS. The CWS decrease of the gNB degrades Wi-Fi performance. To

[4]No other channel sensing-based device can occupy the channel for the 16 μs idle gap. At least an idle period of 25 μs is needed to occupy the channel newly [21].

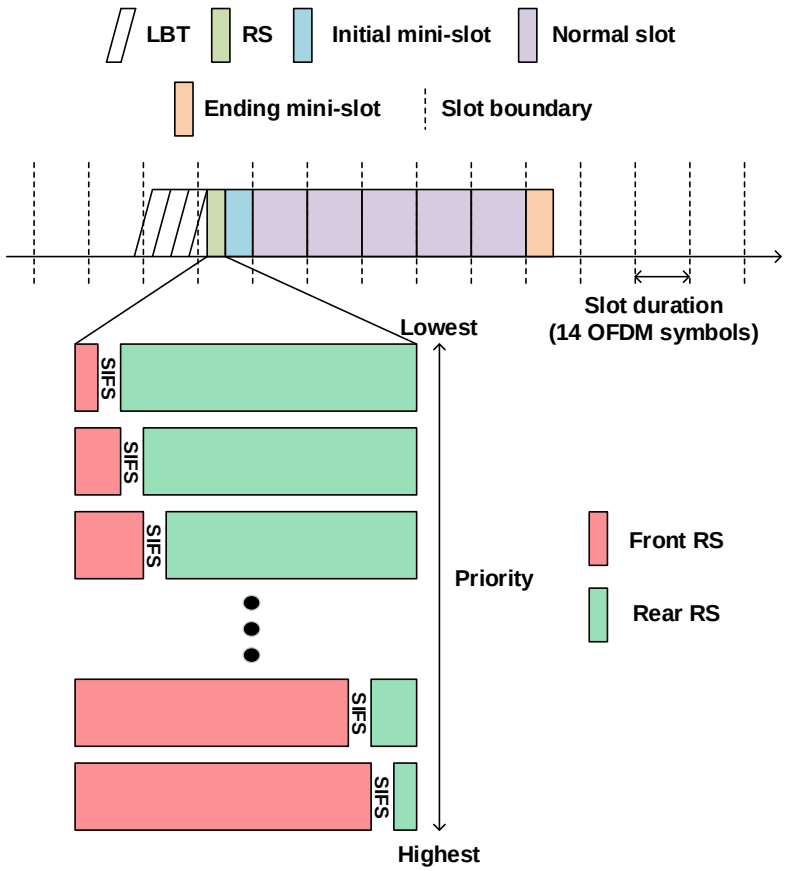

Figure 3.5: New RS structure with a fixed RS duration.

compensate for excessive CWS reduction owing to the new RS operation, each gNB performs the CWS control operation to increase its CWS. For the CWS control, each gNB calculates the conditional probability that its previous successful transmission was resulted from winning a collision. With this probability, it increases its CWS.

3.3.1 New RS structure

When an gNB succeeds in LBT, it calculates the RS duration, d_{RS}, which is the duration from the time that the gNB succeeds in LBT to the next mini-slot starting point.

Using d_{RS}, the gNB obtains the number of RS types, n_{RS}, that the gNB can have, as

$$n_{RS} = \left\lfloor \frac{d_{RS}}{d_{\text{SIFS}}} \right\rfloor, \tag{3.1}$$

where d_{SIFS} is SIFS duration. n_{RS} ranges from 0 to 4 because the maximum RS duration is 71 μs when subcarrier spacing is 30 kHz. The n_{RS} in this range is not a sufficient number for collision resolution. Therefore, the gNB sets a desired n_{RS} value guaranteed for each transmission (X) and extends the RS to obtain this value.

There are two RS extension methods for guaranteeing X. When the expected RS duration can be satisfied by reducing the length of the mini-slot, the length of the initial mini-slot is reduced and the RS is extended accordingly. If not, the current initial mini-slot is changed to RS, and the length of the first normal slot is changed to mini-slots, and then RS is additionally extended.

Fig. 3.5 shows our new RS structure with a fixed RS duration. There is no overlapped idle gap between the two different RS types. We give a different priority to each RS type. As shown in Fig. 3.5, the shorter the front RS duration, the lower the priority of RS type. The gNB randomly selects one RS type that becomes the gNB's priority and accordingly transmits its front RS. If there is no collision, the gNB transmits its rear RS and data slots after having the idle gap of SIFS duration.

When gNBs with different priorities collide during the front RS transmission, the gNB with the highest priority continues to transmit its front RS (which length is longer than that of an gNB with a lower priority) and sense the channel for the SIFS duration. The channel will be idle because the other gNBs with lower priorities have stopped transmission after transmitting their front RS. Then the gNB is allowed to transmit its rear RS and following data slots. This means that the gNB with the highest priority wins the collision, so the collision is resolved.

If there are multiple gNBs with the highest priority in a collision, they all transmit their rear RS and data slots because they have an idle gap of SIFS duration at the same time, sensing the channel idle together. Due to the collision, no gNB receives an ACK,

and the collision is not resolved.

3.3.2 CWS control

The new RS operation reduces collisions by helping each gNB to avoid collisions. For the same example of colliding three gNBs, in the baseline scheme, each gNB receives a NACK and increases its CWS. In our proposal, gNB 2 wins the collision without noticing there was a collision. After gNB 2 succeeds in transmission, it is supposed to use CW_{min} next time, and gNBs 1 and 3 increase their CWS because they have detected a collision. Our CWS control allows the winner to increase its CWS as much as close to the CWS in the baseline scheme. That is, gNB 2 calculates the probability p_{win} that there was a collision and it was the winner. With this probability, gNB 2 increases its CWS, which helps to achieve a good balance between NR-U gNBs and Wi-Fi stations.

To get p_{win}, an gNB first finds out the number n of contending nodes in the saturated channel. Through primary synchronization signal (PSS) and secondary synchronization signal (SSS) decoding, the gNB counts the number of cell IDs of each NR-U transmission. Then we get n and obtain p_{win} as

$$p_{win}(k, n_{RS}) = \frac{\sum_{i=1}^{n-1} \binom{n-1}{i} \tau^i (1-\tau)^{n-1-i} p_i(k, n_{RS})}{\sum_{i=0}^{n-1} \binom{n-1}{i} \tau^i (1-\tau)^{n-1-i} p_i(k, n_{RS})}, \tag{3.2}$$

where k is the priority of the gNB, τ is the measured transmission probability of the gNB defined in Bianchi model [23], and $p_i(k, n_{RS})$ is the probability that the gNB has higher priority than all the other i transmitting gNBs. $p_i(k, n_{RS})$ equals the probability that each of i gNBs selects an RS with a priority lower than k. We define $p_i(k, n_{RS})$ as

$$p_i(k, n_{RS}) = \left(\frac{k-1}{n_{RS}} \right)^i. \tag{3.3}$$

$p_{win}(k, n_{RS})$ is the conditional probability that the gNB receives an ACK as a collision winner when receiving an ACK. If the gNB receives an ACK, it increases its CWS with

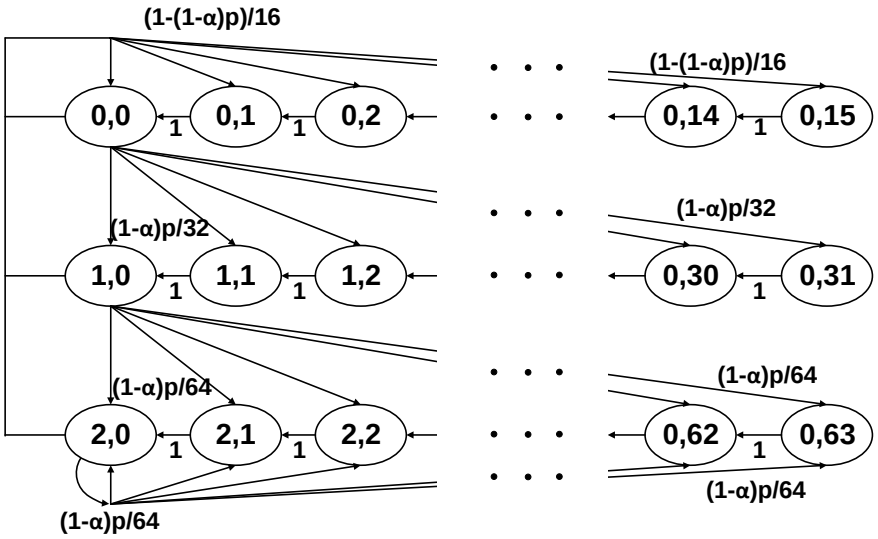

Figure 3.6: An example of the Markov chain model for *R-Split*.

probability $p_{win}(k, n_{RS})$ and uses CW_{min} with probability $(1 - p_{win}(k, n_{RS}))$.

3.4 Performance Analysis

In this section, we mathematically analyze the performance of *R-Split* and *R-SplitC* in an NR-U only network.

3.4.1 Throughput Analysis for R-Split

We analyze the performance of *R-Split* based on [23, 27, 42]. We assume that 1) saturated traffic, and 2) ideal channel (i.e., zero bit error rate (BER)). According to [27], in the LTE-LAA only network, the EPS type of the current transmission and a minimum backoff counter value after the current transmission (bc_{min}) determine the EPS type of subsequent transmission. This feature is the same in the NR-U only network. The only difference between the NR-U only network and the LTE-LAA only network is that there are 13 types of ending mini-slots for NR-U and 7 types of EPS types for LTE-LAA.

We propose a modified Markov chain model to deal with the collision resolution effect of the new RS structure. Then, we derive the steady state EMS type distribution and the network throughput of the system. Fig. 3.6 shows an example of the modified Markov chain model for *R-Split* when the channel access priority class is 3.[5] In the modified Markov chain model, each state (i,j) represents the backoff stage i and the backoff counter value j [23]. p is the probability that the transmission of an gNB results in a collision, the same as in Bianchi model. α is the probability that the gNB selects an RS with the highest priority among the gNBs involved in a collision, and any other gNB does not select the same highest priority. In our scheme, an gNB that participates in a collision and wins the collision uses the minimum CWS next. Due to this property, we replace p with $(1-\alpha)p$ (i.e., reduced collision probability) in the modified Markov chain model.

We use an iterative procedure to get α in the modified Markov chain model. First, we select α_{init} as an input value. Then, we get τ and p by solving the system of equations below.[6]

$$\tau = \frac{2(1-2\bar{\alpha}p)}{(1-2\bar{\alpha}p)(W+1)+\bar{\alpha}pW(1-(2\bar{\alpha}p)^m)}, \tag{3.4}$$

$$p = 1-(1-\tau^{n-1}), \tag{3.5}$$

where $\bar{\alpha} = 1-\alpha_{\text{init}}$. We obtain (3.4) and (3.5) from the modified Markov model based on [23], W is the minimum CWS, m is the maximum backoff stage, and n is the number of contending nodes. Using the results of the modified Markov chain model, we get the bc_{min} distribution.

We define a new bc_{min} distribution of *R-Split* in (3.6) based on [42]. We consider three cases for bc_{min}: successful transmission, resolved collision, and unresolved collision. P_{tr} is the probability that at least one gNB transmits at a generic slot, P_s is the probability that only one gNB transmits when the channel is busy. P_i is the probability

[5] When the channel access priority class is 3, the minimum CWS is 16, and the maximum CWS is 64 [1].

[6] τ is the probability that an gNB transmits at a randomly chosen slot [23].

that i gNBs transmits simultaneously in a generic slot. S_v, B_v, and C_v are the sum of backoff counter value distribution from v to CW_{max} of an gNB that is in the state of successful transmission, idle, and collision, respectively [42]. S_v is defined as

$$S_v = \sum_{l=v}^{CW_{\text{max}}} h_l, \tag{3.7}$$

where h_l is the probability that a gNB station has a backoff counter value l right after its successful transmission. h_l is defined as

$$h_l = \begin{cases} \frac{1}{CW_{\text{min}}+1}, & 0 \leq l \leq CW_{\text{min}}, \\ 0, & l > CW_{\text{min}}, \end{cases} \tag{3.8}$$

where CW_{min} is the NR-U's minimum contention window. B_v is defined as

$$B_v = \sum_{l=v}^{CW_{\text{max}}} g_l, \tag{3.9}$$

where g_l is the probability that a gNB station has a backoff counter value l when the other nodes end transmissions. g_l is defined as

$$g_l = \frac{\sum_{i=0}^{m} b_{i,l+1}}{1 - \sum_{i=0}^{m} b_{i,0}}, \tag{3.10}$$

where $b_{i,k}$ is the stationary distribution that a gNB has the backoff stage i and the backoff counter value k, and m is the maximum backoff stage in the Bianchi model.

$$\begin{aligned} \Pr\left(bc_{\text{min}} = v\right) =& P_s \left(S_v B_v^{n-1} - S_{v+1} B_{v+1}^{n-1}\right) \\ &+ \sum_{i=2}^{n} \frac{P_i}{P_{tr}} \left[\delta_i \left(S_v C_v^{i-1} B_v^{n-i} - S_{v+1} C_{v+1}^{i-1} B_{v+1}^{n-i}\right)\right. \\ &\left. + \left(1 - \delta_i\right) \left(C_v^i B_v^{n-i} - C_{v+1}^i B_{v+1}^{n-i}\right)\right]. \end{aligned} \tag{3.6}$$

C_v is defined as

$$C_v = \sum_{l=v}^{CW_{\text{max}}} w_l, \tag{3.11}$$

where w_l is the probability that a gNB has a backoff counter value l after experiencing a collision. w_l is defined as

$$w_l = \frac{\sum_{i=i_s}^{m-1} \left(\frac{b_{i,0}}{2^{i+1}(CW_{\text{min}}+1)} \right) + \frac{b_{m,0}}{CW_{\text{max}}+1}}{\sum_{i=0}^{m} b_{i,0}}, \tag{3.12}$$

where $i_s = \max\left(\lfloor log_2 l \rfloor - log_2(CW_{\text{min}}+1), 0\right)$. δ_i is the collision resolution probability from the network perspective when the number of gNBs included in the collision is i. We define δ_i as

$$\delta_i = \sum_{x=1}^{X-1} \left[i \left(\frac{1}{X} \right) \left(\frac{x}{X} \right)^{i-1} \right], \tag{3.13}$$

where X is the fixed number of RS types. δ_i is the same as the probability that there is only one highest number when i nodes each select one number from 1 to X by allowing duplicates.

We update α_{init} as

$$\alpha_{\text{init}} = \frac{\sum_{i=2}^{n} \frac{P_i}{P_c} \delta_i}{\sum_{i=2}^{n} \frac{P_i}{P_c} i}, \tag{3.14}$$

where P_c is the probability that the channel is in the collision state in a slot. Updated α_{init} is equal to the number of resolved collisions divided by the number of total transmissions involved in collisions. With the updated α_{init}, we repeat the iteration. After a few iterations, we obtain converged τ, α, and bc_{min}.[7] We calculate the steady state EMS type distribution using bc_{min}. Based on [27], we obtain the steady state EMS type distribution π by solving

$$\pi \mathbf{P} = \pi, \tag{3.15}$$

[7] In Section 3.5, we use five iterations to obtain analysis results.

Table 3.1: Transition matrix **P** from state i to state j (priority class = 3 and subcarrier spacing = 30 kHz)

$i \backslash j$	1	2	3	4	5	6	7	8	9	10	11	12	13
1	[0,3],[51,58]	[4,7],[59,62]	[8,10],63	[11,14]	[15,18]	[19,22]	[23,26]	[27,30]	[31,34]	[35,38]	[39,42]	[43,46]	[47,50]
2	[43,50]	[51,54]	[0,3],[55,58]	[4,7],[59,62]	[8,11],63	[12,15]	[16,18]	[19,22]	[23,26]	[27,30]	[31,34]	[35,38]	[39,42]
3	[39,46]	[47,50]	[51,54]	[0,3],[55,58]	[4,7],[59,62]	[8,11],63	[12,14]	[15,18]	[19,22]	[23,26]	[27,30]	[31,34]	[35,38]
4	[35,42]	[43,46]	[47,50]	[51,54]	[0,3],[55,58]	[4,7],[59,62]	[8,11],63	[12,14]	[15,18]	[19,22]	[23,26]	[27,30]	[31,34]
5	[31,38]	[39,42]	[43,46]	[47,50]	[51,54]	[0,3],[55,58]	[4,7],[59,62]	[8,11],63	[12,15]	[16,18]	[19,22]	[23,26]	[27,30]
6	[27,34]	[35,38]	[39,42]	[43,46]	[47,50]	[51,54]	[0,3],[55,58]	[4,7],[59,62]	[8,11],63	[12,14]	[15,18]	[19,22]	[23,26]
7	[23,30]	[31,34]	[35,38]	[39,42]	[43,46]	[47,50]	[51,54]	[0,3],[55,58]	[4,7],[59,62]	[8,10],63	[11,14]	[15,18]	[19,22]
8	[20,26]	[27,30]	[31,34]	[35,38]	[39,42]	[43,46]	[47,50]	[51,54]	[0,3],[55,58]	[4,7],[59,62]	[8,11],63	[12,15]	[16,19]
9	[16,22]	[23,26]	[27,30]	[31,34]	[35,38]	[39,42]	[43,46]	[47,50]	[51,54]	[0,3],[55,58]	[4,7],[59,62]	[8,11],63	[12,15]
10	[12,18]	[19,22]	[23,26]	[27,30]	[31,34]	[35,38]	[39,42]	[43,46]	[47,50]	[51,54]	[0,3],[55,58]	[4,7][59,62]	[8,11],63
11	[8,15],63	[16,19]	[20,22]	[23,26]	[27,30]	[31,34]	[35,38]	[39,42]	[43,46]	[47,50]	[51,54]	[0,3],[55,58]	[4,7],[59,62]
12	[4,11],[59,63]	[12,15]	[16,18]	[19,22]	[23,26]	[27,30]	[31,34]	[35,38]	[39,42]	[43,46]	[47,50]	[51,54]	[0,3],[55,58]
13	[0,7],[55,62]	[8,11],63	[12,14]	[15,18]	[19,22]	[23,26]	[27,30]	[31,34]	[35,38]	[39,42]	[43,46]	[47,50]	[51,54]

where **P** is the transition matrix. Table 3.1 shows an example of **P** when the priority class is 3 and subcarrier spacing is 30 kHz.[8]

Based on the Bianchi model and [27], we define the estimated throughput of the modified Markov chain model as

$$E[S] = \frac{(P_s P_{tr} + \sum_{i=2}^{n} P_i \delta_i) E[B]}{(1 - P_{tr})\sigma + P_{tr} E[T]}, \tag{3.16}$$

where σ is the clear channel assessment (CCA) slot duration, $E[T]$ is the average transmission duration, and $E[B]$ is the average transmitted bits in a successful transmission. In the baseline scheme, successful transmission occurs when no collision has occurred. In our scheme, however, a successful transmission can occur even if there is a collision. We reflect this difference in the numerator of (3.16).

We define $E[T]$ as

$$E[T] = \left(\sum_{j=1}^{13} \sum_{v=0}^{CW_{\max}} \Pr(\text{EMS type} = j) \Pr(bc_{\min} = v) T(j, v) \right) + d_{\text{AIFS}}, \tag{3.17}$$

where $T(j, v)$ is the transmission duration when EMS type of the previous transmission is j the minimum backoff counter value is v and d_{AIFS} is duration of AIFS.[9] We

[8] Each component [a,b] means that EMS type i transitions to EMS type j when the $bc_{\min}$ value is between a and b.

[9] In Bianchi model, defer period is contained in a transmission slot.

define $T(j, v)$ as

$$T(j, v) = d_{\text{rs}}(j, v) + d_{\text{ims}}(j, v) + d_{\text{slot}} n_{\text{slot}}(j, v) + d_{\text{ems}}(j, v), \tag{3.18}$$

where $d_{\text{rs}}(j, v)$ is an RS duration for given j and v, $d_{\text{ims}}(j, v)$ is an initial mini-slot duration for given j and v, d_{slot} is a slot duration determined by subcarrier spacing, $n_{\text{slot}}(j, v)$ is the number of normal slots in the transmission for given j and v, and $d_{\text{ems}}(j, v)$ is an ending mini-slot duration for given j and v. When j and v are given, we define $d_{\text{nsb}}(j, v)$ as the duration between the LBT success time and the next slot boundary. Then, we determine an initial mini-slot that has a maximum duration shorter than $d_{\text{nsb}}(j, v)$ among the 13 initial mini-slot types (including no initial mini-slot case). $d_{\text{ims}}(j, v)$ is the duration of the selected initial mini-slot. Then, $d_{\text{rs}}(j, v)$ is

$$d_{\text{rs}}(j, v) = d_{\text{nsb}}(j, v) - d_{\text{ims}}(j, v). \tag{3.19}$$

We define $n_{\text{slot}}(j, v)$ as

$$n_{\text{slot}}(j, v) = \Big\lfloor \frac{d_{\text{mcot}} - d_{\text{rs}}(j, v) - d_{\text{ims}}(j, v)}{d_{\text{slot}}} \Big\rfloor, \tag{3.20}$$

where d_{mcot} is the duration of MCOT. Then, we determine an ending mini-slot that has a maximum duration shorter than $d_{\text{mcot}} - d_{\text{rs}}(j, v) - d_{\text{ims}}(j, v) - d_{\text{slot}} n_{\text{slot}}(j, v)$ among the 13 ending mini-slot types (including no ending mini-slot case).

When $d_{\text{rs}}(j, v)$ is short for generating X RS types, we extend the RS duration for guaranteeing X RS types. As the RS duration is extended, $d_{\text{rs}}(j, v)$, $d_{\text{ims}}(j, v)$, and $n_{\text{slot}}(j, v)$ become $d^*_{\text{rs}}(j, v)$, $d^*_{\text{ims}}(j, v)$, and $n^*_{\text{slot}}(j, v)$, respectively. When $d_{\text{rs}}(j, v) + d_{\text{ims}}(j, v)$ is longer than $d_{\text{SIFS}} \cdot X$, RS extension is performed in the initial mini-slot. In this case, we determine a new initial mini-slot that has a maximum duration shorter than $d_{\text{rs}}(j, v) + d_{\text{ims}}(j, v) - (d_{\text{SIFS}} \cdot X)$ among the 13 initial mini-slot types (including no initial mini-slot case). $d^*_{\text{ims}}(j, v)$ is the duration of the new initial mini-slot. Then

$d^*_{\text{rs}}(j,v)$ becomes $d_{\text{rs}}(j,v) + d_{\text{ims}}(j,v) - d^*_{\text{ims}}(j,v)$.

On the other hand, when $d_{\text{rs}}(j,v)+d_{\text{ims}}(j,v)$ is shorter than $d_{\text{SIFS}}\cdot X$, RS extension is performed until the first normal slot. In this case, $n^*_{\text{slot}}(j,v)$ becomes $n_{\text{slot}}(j,v)-1$.[10] we also determine a new initial mini-slot that has a maximum duration shorter than $d_{\text{rs}}(j,v)+d_{\text{ims}}(j,v)+d_{\text{slot}}-(d_{\text{SIFS}}\cdot X)$ among the 13 initial mini-slot types (including no initial mini-slot case). $d^*_{\text{ims}}(j,v)$ is the duration of the new initial mini-slot. Then $d^*_{\text{rs}}(j,v)$ becomes $d_{\text{rs}}(j,v) + d_{\text{ims}}(j,v) + d_{\text{slot}} - d^*_{\text{ims}}(j,v)$. With the newly defined $d^*_{\text{rs}}(j,v)$, $d^*_{\text{ims}}(j,v)$, and $n^*_{\text{slot}}(j,v)$, we can refine $T(j,v)$ as

$$T(j,v) = d^*_{\text{rs}}(j,v) + d^*_{\text{ims}}(j,v) + d_{\text{slot}}n^*_{\text{slot}}(j,v) + d_{\text{ems}}(j,v). \tag{3.21}$$

We define $E[B]$ as

$$E[B] = \sum_{j=1}^{13}\sum_{v=0}^{CW_{\text{max}}} \Pr(\text{EMS type} = j)\Pr(bc_{\text{min}} = v)\, B(j,v), \tag{3.22}$$

where $B(j,v)$ is the transmitted information bits when EMS type of the previous transmission is j and the minimum backoff counter value is v. we define $B(j,v)$ as

$$B(j,v) = B_{\text{ims}^*} + B_{\text{slot}}n^*_{\text{slot}}(j,v) + B_{\text{ems}}, \tag{3.23}$$

where B_{ims^*} is the transmitted information bits at the new initial mini-slot, B_{slot} is the transmitted information bits at a normal slot, and B_{ems^*} is the transmitted information bits at the ending mini-slot.

3.4.2 Throughput Analysis for R-SplitC

We analyze the performance of *R-SplitC* in the NR-U only network based on [23, 27, 42]. We use the same assumptions as in the previous subsection.

Our CWS control operation additionally increases the CWS of an gNB with a

[10] More than one slots can be used for RS extension. In the dissertation, we only consider one slot.

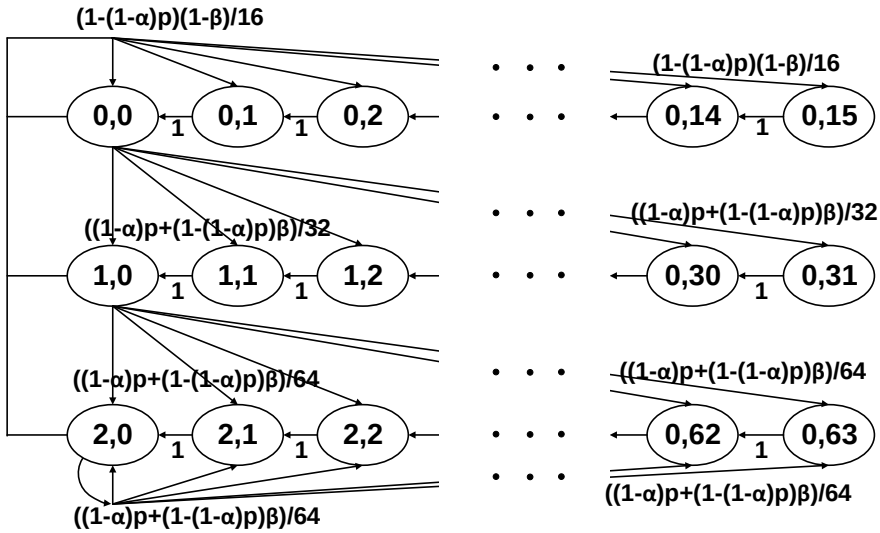

Figure 3.7: An example of Markov chain model for *R-SplitC*.

specific probability when it receives an ACK. For *R-SplitC* modeling, we modify the Markov chain model of *R-Split* by expressing this probability as β, as shown in Fig. 3.7, when the channel access priority class is 3. If an gNB transmits a frame successfully in *R-Split*, the gNB's backoff stage becomes zero with probability $(1-(1-\alpha)p)$. In *R-SplitC*, if an gNB transmits a frame successfully, the gNB's backoff stage becomes zero with probability $(1-(1-\alpha)p)(1-\beta)$.

To get α and β, we use an iterative procedure similar to that used in the analysis of *R-Split*. First, we select α_{init} and β_{init} as input values. Then, we get τ and p through the modified Markov chain model. We obtain τ and p by solving the system of equations below.

$$\tau = \frac{2(1-2\bar{\beta}p)}{(1-2\bar{\beta}p)(W+1)+\bar{\beta}pW(1-(2\bar{\beta}p)^m)}, \tag{3.24}$$

$$p = 1-(1-\tau)^{n-1}, \tag{3.25}$$

where $\bar{\beta} = \beta_{\text{init}} + (1-\alpha_{\text{init}})(1-\beta_{\text{init}})p$ in (3.24). Using the results of the modified Markov chain model, we get a new bc_{min} distribution.

We define a new bc_{min} distribution of *R-SplitC* in (3.26), where β is the probability

that the gNB increases CWS when it receives an ACK. When β is zero, (3.26) becomes (3.6).

We update α_{init} by using (3.14) and β_{init} as

$$\beta_{\text{init}} = \frac{\sum_{i=1}^{n-1} \binom{n-1}{i} \tau^i (1-\tau)^{n-1-i} p_i}{\sum_{i=0}^{n-1} \binom{n-1}{i} \tau^i (1-\tau)^{n-1-i} p_i}, \tag{3.27}$$

where p_i is the probability that all the other i nodes select lower priorities than the gNB. We define p_i as

$$p_i = \begin{cases} \sum_{x=1}^{X-1} \left[\left(\frac{1}{X}\right) \left(\frac{x}{X}\right)^{i-1} \right], & i > 0, \\ 1, & i = 0. \end{cases} \tag{3.28}$$

With the updated α_{init} and β_{init}, we repeat the iteration. After a few iterations, we get converged τ, α, β, and bc_{min2}. With these converged parameters, we calculate the network throughput of *R-SplitC* using (3.16)–(3.23). The difference between *R-Split* and *R-SplitC* is that they use bc_{min} and bc_{min2} distributions, respectively.

3.5 Performance Evaluation

In this section, we validate the analysis results for our proposed schemes in an NR-U only network, and evaluate their performance in NR-U only and NR-U with Wi-Fi network environments. We implemented NR-U simulator and NR-U/Wi-Fi coexistence

---

$$\begin{aligned} \Pr\left(bc_{\text{min2}} = v\right) =& P_s \left(1-\beta\right) \left(S_v B_v^{n-1} - S_{v+1} B_{v+1}^{n-1}\right) \\ &+ P_s \beta \left(C_v B_v^{n-1} - C_{v+1} B_{v+1}^{n-1}\right) \\ &+ \sum_{i=2}^{n} \frac{P_i}{P_{tr}} \left[\delta_i \left(1-\beta\right) \left(S_v C_v^{i-1} B_v^{n-i} - S_{v+1} C_{v+1}^{i-1} B_{v+1}^{n-i}\right)\right. \\ &+ \delta_i \beta \left(C_v^i B_v^{n-i} - C_{v+1}^i B_{v+1}^{n-i}\right) \\ &+ \left.\left(1-\delta_i\right) \left(C_v^i B_v^{n-i} - C_{v+1}^i B_{v+1}^{n-i}\right)\right]. \end{aligned} \tag{3.26}$$

Table 3.2: Simulation parameters for an NR-U only network.

Parameter	Value
SIFS	16 μs
AIFS	43 μs
MCOT	10 ms
NR-U CW_{min}	15
NR-U CW_{max}	63
Bandwidth	20 MHz
NR-U MCS	28

simulator with MATLAB. We conducted simulations in a topology where nodes are randomly distributed in a circle with a radius of 25 m. We simulated 10^6 transmissions. We implemented an ideal channel where transmission failures are caused only by collisions and used fixed MCS for the NR-U only network to compare with the analysis result. We implemented the 3GPP urban micro (UMi) path loss model and adaptive modulation and coding scheme (AMC) for the NR-U/Wi-Fi network for more realistic environment. We set the maximum MCOT and A-MPDU duration in the standard. Other detailed simulation parameters are summarized in Tables 3.2 and 3.3.

For performance comparison, we consider two schemes: 1) The baseline operation of NR-U, which uses RS only for channel reservation and 2) CR-LBT, which uses an RS as collision resolution [40].

3.5.1 Performance Evaluation for an NR-U only Network

Fig. 3.8 shows the network throughput of *R-Split*. The number after *R-Split* means the number of RS types guaranteed through RS extension. The gap between simulation and analysis results of *R-Split* is merely 0.04% on average. In the baseline, network throughput greatly decreases as the number of contending nodes increases. This is because the damage caused by the increasing collision is getting bigger. CR-LBT shows almost similar performance to the baseline. This is because the RS duration in NR-U is too short to show collision resolution performance. *R-Split* shows the best perfor-

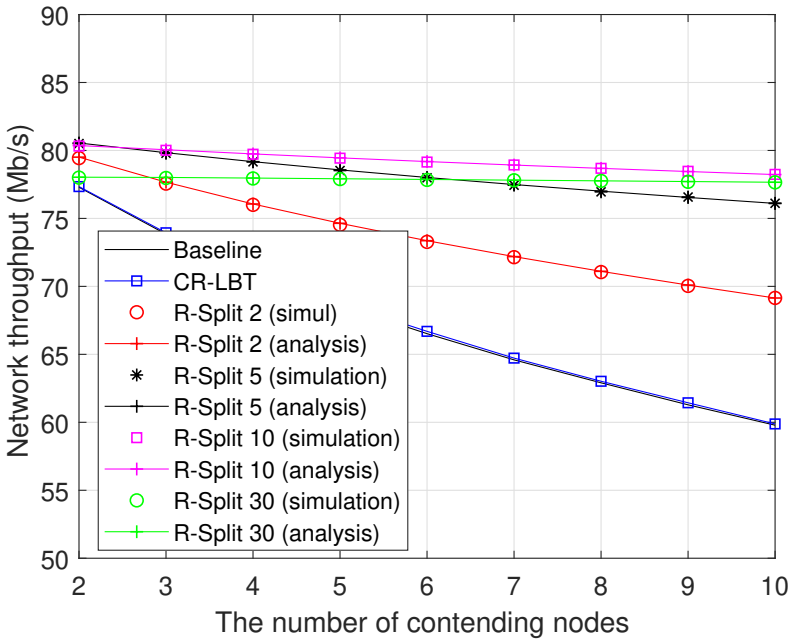

Figure 3.8: Network throughput of *R-Split*.

mance when the number of guaranteed RS types is 10. If the number of guaranteed RS types is too small, the performance of collision resolution is poor. On the contrary, if the number of RS types is too large, the overhead due to the reduction of the data slot is greater than the increase in the performance of the collision resolution. Therefore, using an appropriate number of RS types shows the best results. Compared to the baseline scheme and CR-LBT, *R-Split* 10 shows the throughput gain of 30.86% and 30.66% when the number of contending nodes is 10, respectively.

Fig. 3.9 shows the network throughput of *R-SplitC*. The difference between simulation and analysis results is merely 0.05% on average. The overall trend of *R-SplitC* is the same as that of *R-Split*. When the number of guaranteed RS types is 10, the performance of R-SplitC is the best. The performance of *R-SplitC* is slightly higher than that of *R-Split*. This is because the additional CWS increase of *R-SplitC* shows an effect of collision reduction. Compared to the baseline scheme and CR-LBT, *R-SplitC* 10 shows the throughput gain of 31.64% and 31.44% when the number of contending

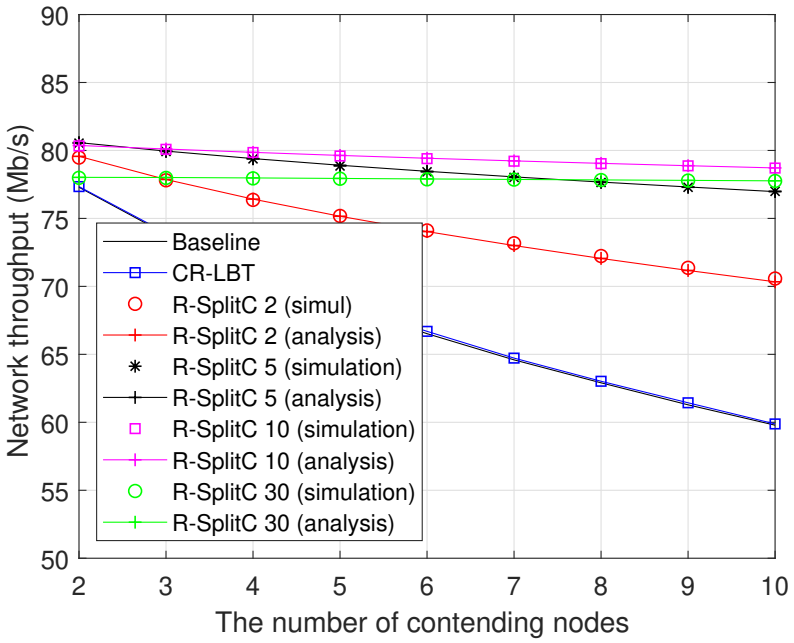

Figure 3.9: Network throughput of *R-SplitC*.

nodes is 10, respectively.

Fig. 3.10 shows the collision time ratio according to the number of contending nodes. In the baseline scheme, the collision time ratio increases with the number of contending nodes. CR-LBT shows similar collision time ratio compared to the baseline scheme due to short RS duration. In contrast, the collision time ratios in our schemes are considerably lower than that in the baseline scheme and CR-LBT, and do not increase significantly even when the number of contending nodes increases. Our schemes successfully avoid collisions by using the new RS structure. *R-splitC* 10 has a slightly lower collision time ratio than *R-split* 10. This is due to the fact that the collision resolution is resolved through *R-Split* operation, but the CWS increase occurs so little that the collision itself increases. *R-SplitC* has a lower collision time ratio because it does not increase collision by calibrating it through the CWS control operation and also takes the collision resolution effect.

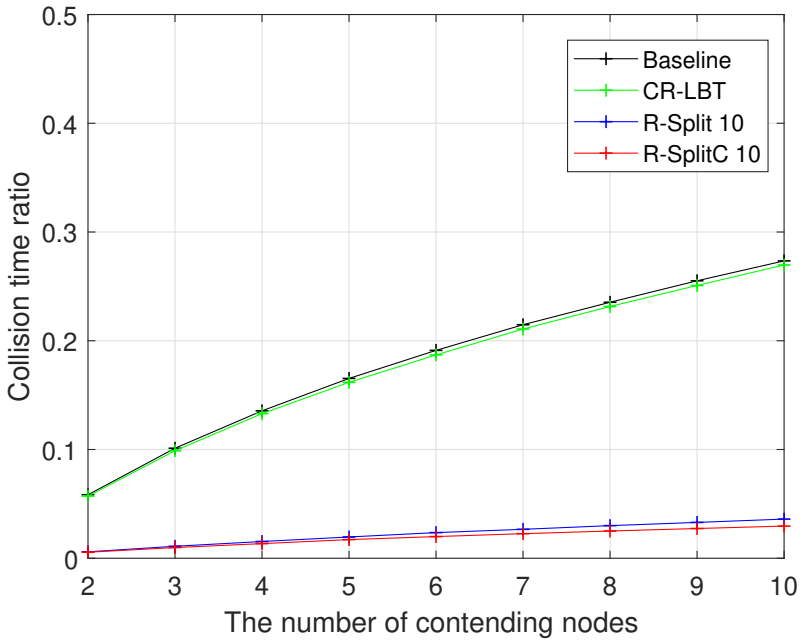

Figure 3.10: Collision time ratio.

3.5.2 Performance Evaluation for an NR-U/Wi-Fi Network.

We evaluate the performance of our proposed schemes under the coexistence of NR-U and Wi-Fi, where NR-U gNBs and Wi-Fi APs coexist in a one-to-one ratio. Fig. 3.11 shows NR-U throughput, Wi-Fi throughput, and sum throughput according to the number of contending nodes when subcarrier spacing is 30 kHz. Wi-Fi APs do not use RTS/CTS. With the number of nodes in the baseline scheme, the throughput of NR-U and Wi-Fi decrease due to increased collisions. In CR-LBT, NR-U slightly decreases and Wi-Fi slightly increases compared with the baseline scheme. This is because only the operation considering Wi-Fi of the CR-LBT sometimes operates due to the short RS duration of NR-U. In *R-SplitC* 10, NR-U throughput is much larger than in the baseline scheme and CR-LBT.

There are two reasons for the NR-U throughput improvement in *R-SplitC* 10. First, *R-SplitC* 10 resolves collisions of NR-U transmissions successfully. Second, due to the

Table 3.3: Simulation parameters for an NR-U/Wi-Fi network

Parameter	Value
SIFS	16 μs
AIFS	43 μs
MCOT	8 ms
NR-U CW_{min}	15
NR-U CW_{max}	63
A-MPDU duration	5.484 ms
Wi-Fi CW_{min}	15
Wi-Fi CW_{max}	1023
Bandwidth	20 MHz
Wi-Fi PHY	802.11ac, SISO
Wi-Fi rate adaptation	Minstrel VHT
NR-U rate adaptation	AMC

collision resolution, MCS underestimation, which occurs each time a collision occurs, occurs less frequently. Thus, the average MCS in our proposed schemes is greater than that in the baseline scheme. *R-SplitC* 10 tries to keep the CWS value of NR-U similar to the baseline scheme, and accordingly, it boosts NR-U performance without sacrificing Wi-Fi performance. When the number of contending nodes is 20, *R-SplitC* 10 increases the NR-U throughput by 136.6% and also increases the Wi-Fi throughput by 4.44% compared to the baseline scheme. As a result, *R-SplitC* 10 increases the overall network throughput by 99.29%.

We evaluate the performance under the coexistence of NR-U and Wi-Fi using RTS/CTS. Fig. 3.12 shows NR-U throughput, Wi-Fi throughput, and sum throughput according to the number of contending nodes when subcarrier spacing is 30 kHz. Compared to the no RTS/CTS case, the throughput gap between NR-U and Wi-Fi becomes larger. This is because when NR-U and Wi-Fi transmissions collide, Wi-Fi transmission stops first due to the decoding failure of RTS frame while NR-U transmission continues. In CR-LBT, NR-U slightly decreases and Wi-Fi slightly increases compared with the baseline scheme as in the no RTS/CTS case. *R-SplitC* 10 increases the throughput of NR-U compared to the baseline scheme. It also maintains almost

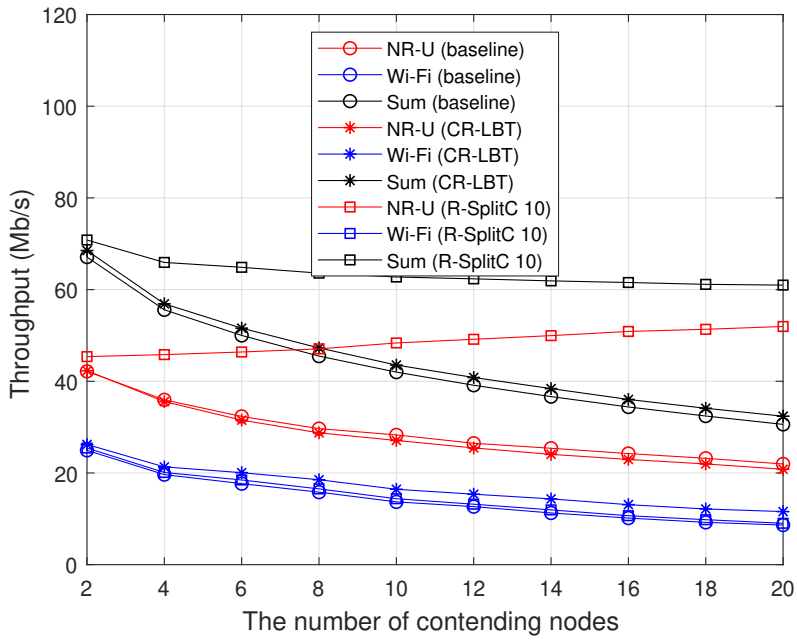

Figure 3.11: Performance of NR-U and Wi-Fi without RTS/CTS (30 kHz subcarrier spacing).

the same Wi-Fi performance as the baseline scheme. When the number of contending nodes is 20, *R-SplitC* 10 increases the throughput of NR-U by 111% and also increases the throughput of Wi-Fi by 0.34% compared to the baseline scheme. *R-SplitC* 10 improves the overall network throughput by 90.3% compared to the baseline.

We evaluate the coexistence performance of NR-U and Wi-Fi in 15 kHz subcarrier spacing environment. As the subcarrier spacing is changed from 30 kHz to 15 kHz, the slot duration increases from 0.5 ms to 1 ms, and the OFDM symbol duration also doubles. That is, the RS duration is also doubled. Fig. 3.13 shows NR-U throughput, Wi-Fi throughput, and sum throughput according to the number of contending nodes when subcarrier spacing is 15 kHz. Wi-Fi APs do not use RTS/CTS. In the baseline scheme, NR-U and Wi-Fi show almost similar performance to 30 kHz subcarrier spacing case. In CR-LBT, Wi-Fi increases compared to 30 kHz subcarrier spacing thanks to increased RS duration. *R-SplitC* 10 shows similar results compared with 30 kHz

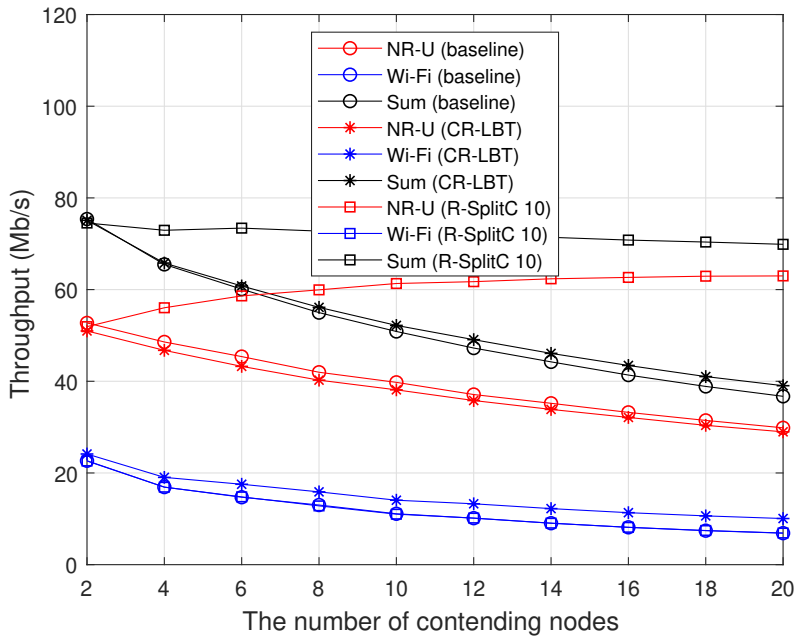

Figure 3.12: Performance of NR-U and Wi-Fi with RTS/CTS (30 kHz subcarrier spacing).

subcarrier spacing. It is because that *R-SplitC* 10 has similar RS duration regardless of subcarrier spacing. When the number of contending nodes is 20, *R-SplitC* 10 increases the throughput of NR-U by 137.1% and also increases the throughput of Wi-Fi by 7.1% compared to the baseline scheme.

Fig. 3.14 shows NR-U throughput, Wi-Fi throughput, and sum throughput according to the number of contending nodes when subcarrier spacing is 15 kHz. Wi-Fi APs use RTS/CTS. In the baseline scheme, NR-U and Wi-Fi show almost similar performance to 30 kHz subcarrier spacing case. In CR-LBT, Wi-Fi increases compared to 30 kHz subcarrier spacing thanks to increased RS duration. *R-SplitC* 10 shows similar results compared with 30 kHz subcarrier spacing. It is because that *R-SplitC* 10 has similar RS duration regardless of subcarrier spacing. When the number of contending nodes is 20, *R-SplitC* 10 increases the throughput of NR-U by 113.6% and also decreases the throughput of Wi-Fi by 2.6% compared to the baseline scheme.

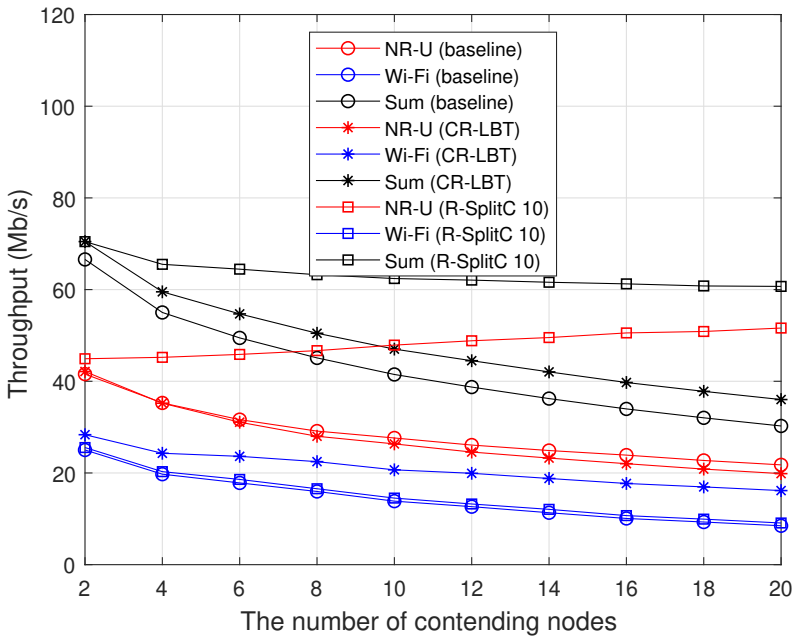

Figure 3.13: Performance of NR-U and Wi-Fi without RTS/CTS (15 kHz subcarrier spacing).

3.6 Summary

In this chapter, we focused on the collision problem that occurs when multiple NR-U gNBs are transmitting at the same time. To solve this problem, we proposed a collision resolution scheme, termed *R-Split*, that aims to minimize the collision probability by introducing a new RS structure. *R-Split* extends RS duration and uses a split RS and place an idle gap of SIFS duration between front and rear RSs to sense the channel in the middle of RS transmissions. Even when an RS collision occurs, *R-Split* enables an NR-U gNB to make a successful transmission. We added a CWS control procedure to *R-Split* to compensate for CWS reduced by *R-Split* and named it as *R-SplitC*, which protects Wi-Fi traffic when NR-U and Wi-Fi traffic coexist. *R-SplitC* allows an gNB winning the contention to increase its CWS probabilistically to provide room for Wi-Fi transmission. Through mathematical analysis and simulation, we confirmed that

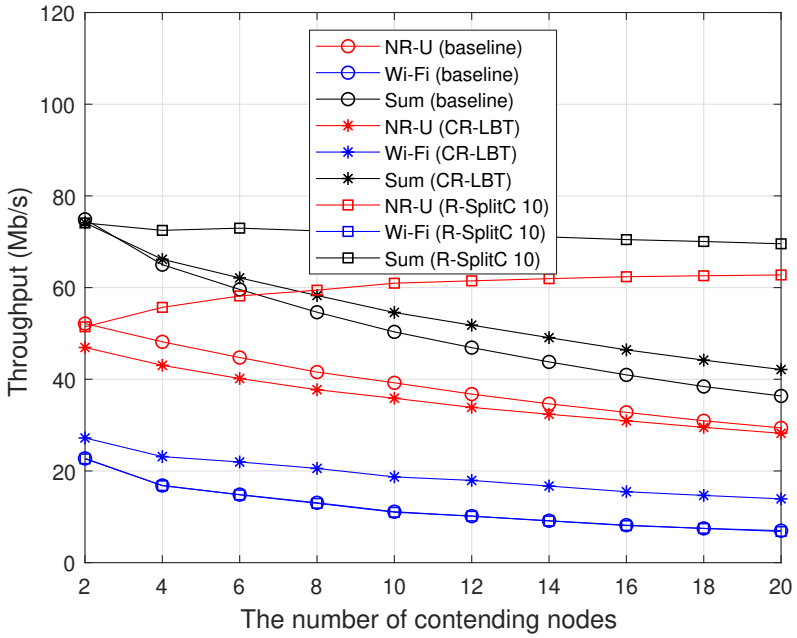

Figure 3.14: Performance of NR-U and Wi-Fi with RTS/CTS (15 kHz subcarrier spacing).

R-SplitC significantly improves the performance of NR-U without sacrificing Wi-Fi performance.

Chapter 4

Concluding Remarks

4.1 Research Contributions

In this dissertation, we have addressed

In Chapter 2, we investigated the uplink channel access problem of cellular communication in the unlicensed spectrum through mathematical analysis, and proposed a standard-compliant solution named UpChance. The UE in UpChance uses a minimum length of uplink reservation signal for contention-based channel access, without harming the nature of UL multi-access. The eNB in UpChance detects channel saturation and schedules the UE's uplink transmission with the best delay. Through ns-3 simulation, we evaluated the performance of UpChance in UL data transmission and random access scenarios. We confirmed that UpChance achieves fairness performance improvement of up to 88% in the UL data scenario, and the random access completion time gain of up to 99% in the random access scenario.

In Chapter 3, we focused on the collision problem that occurs when multiple NR-U gNBs are transmitting at the same time. To solve this problem, we proposed a collision resolution scheme, termed *R-Split*, that aims to minimize the collision probability by introducing a new RS structure. *R-Split* extends RS duration and uses a split RS and place an idle gap of SIFS duration between front and rear RSs to sense the channel in

the middle of RS transmissions. Even when an RS collision occurs, *R-Split* enables an NR-U gNB to make a successful transmission. We added a CWS control procedure to *R-Split* to compensate for CWS reduced by *R-Split* and named it as *R-SplitC*, which protects Wi-Fi traffic when NR-U and Wi-Fi traffic coexist. *R-SplitC* allows an gNB winning the contention to increase its CWS probabilistically to provide room for Wi-Fi transmission. Through mathematical analysis and simulation, we confirmed that *R-SplitC* significantly improves the performance of NR-U without sacrificing Wi-Fi performance.

4.2 Future Work

As further improvement on the results of this dissertation, there are several research items as follows.

First, UpChance operates well when the UE uses 25 μs LBT for uplink transmission. We plan to extend UpChance to operation in the other environment such as autonomous uplink in feLAA and configured grant in NR-U.

Second, we use the fixed number of RS types in *R-SplitC*. We plan to adapt the optimal number of guaranteed RS types of *R-SplitC* according to the environment.

Lastly, our performance analysis focused on the NR-U only network. We plan to analyze the coexistence performance of NR-U and Wi-Fi of *R-Split* and *R-SplitC*.

Bibliography

[1] 3GPP TS 36.213 V13.0.1, *Evolved universal terrestrial radio access (E-UTRA) physical layer procedures (Release 13)*, 3GPP, 2016.

[2] 3GPP TS 36.214 V14.0.0, *Evolved universal terrestrial radio access (E-UTRA) physical layer procedures (Release 14)*, 3GPP, 2016.

[3] 3GPP TS 36.215 V15.0.0, *Evolved universal terrestrial radio access (E-UTRA) physical layer procedures (Release 15)*, 3GPP, 2017.

[4] B. Kang, S. Choi, S. Jung, and S. Bahk, "D2d communications underlaying cellular networks on licensed and unlicensed bands with qos constraints," *IEEE J. Commun. Netw.*, no. 99, pp. 1–13, 2019.

[5] MulteFire Release 1.0 Technical Paper, *A New Way to Wireless*, MulteFire Alliance, 2017.

[6] 3GPP TR 38.889 V16.0.0, *Study on NR-based access to unlicensed spectrum (Release 16)*, 3GPP, 2018.

[7] H. Song, Q. Cui, Y. Gu, G. L. Stüber, Y. Li, Z. Fei, and C. Guo, "Cooperative lbt design and effective capacity analysis for 5g nr ultra dense networks in unlicensed spectrum," *IEEE Access*, vol. 7, pp. 50 265–50 279, 2019.

[8] L. H. Vu and J.-H. Yun, “Adaptive self-deferral for carrier aggregation of lte-laa with rf power leakage in unlicensed spectrum,” *IEEE Access*, vol. 7, pp. 89 292–89 305, 2019.

[9] IEEE 802.11 Coexistence Workshop Agenda - DRAFT 2.0”. [Online]. Available: https://grouper.ieee.org/groups/802/11/Workshops/2019-July-Coex/2019-07-Coex-agenda-2.htm

[10] V. Sathya, M. I. C. Rochman, and M. Ghosh, “Impact of changing energy detection thresholds on fair coexistence of wi-fi and lte in the unlicensed spectrum,” in *Proc. IEEE WTS*, 2017, pp. 1–9.

[11] E. Chai, K. Sundaresan, M. A. Khojastepour, and S. Rangarajan, “Lte in unlicensed spectrum: Are we there yet?” in *Proc. ACM MobiCom*, 2016, pp. 135–148.

[12] Q. Chen, G. Yu, and Z. Ding, “Enhanced laa for unlicensed lte deployment based on txop contention,” *IEEE Trans. Commun.*, vol. 67, no. 1, pp. 417–429, 2018.

[13] Q. Chen and Z. Ding, “On non-intrusive coexistence of elaa and legacy wifi networks,” in *Proc. IEEE ICC*, 2019, pp. 1–6.

[14] S.-T. Hong, H. Lee, H. Kim, and H. J. Yang, “Lightweight wi-fi frame detection for licensed assisted access lte,” *IEEE Access*, vol. 7, pp. 77 618–77 628, 2019.

[15] K. Yoon, T. Park, J. Kim, W. Sun, S. Hwang, I. Kang, and S. Choi, “Cota: Channel occupancy time adaptation for lte in unlicensed spectrum,” in *Proc. IEEE DySPAN*, 2017, pp. 1–10.

[16] R. Karaki, J.-F. Cheng, E. Obregon, A. Mukherjee, S. Falahati, H. Koorapaty, O. Drugge *et al.*, “Uplink performance of enhanced licensed assisted access (elaa) in unlicensed spectrum,” in *Proc. IEEE WCNC*, 2017, pp. 1–6.

[17] R. K. Sheshadri, K. Sundaresan, E. Chai, A. Khojastepour, S. Rangarajan, and D. Koutsonikolas, “Blu: Blue-printing interference for robust lte access in unlicensed spectrum,” in *Proc. ACM CoNEXT*, 2017, pp. 15–27.

[18] V. Sathya, A. Ramamurthy, M. I. Rochman, and M. Ghosh, “Qos guaranteed radio resource scheduling in stand-alone unlicensed multefir,” in *Proc. IEEE 5GWF*, 2020, pp. 86–91.

[19] A. Mbengue and Y. Chang, “Space-time domain analysis for enhanced laa uplink/wi-fi coexistence: Random or scheduled access,” *IEEE Access*, vol. 7, pp. 41 470–41 478, 2019.

[20] F. D. Tilahun and C. G. Kang, “Decentralized deep reinforcement learning-based dynamic uplink band selection in enhanced licensed-assisted access,” in *Proc. IEEE ICOIN*, 2020, pp. 477–480.

[21] Final draft ETSI EN 301 893 V2.1.0, *Harmonised Standard covering the essential requirements of article 3.2 of Directive 2014/53/EU*, ETSI, 2017.

[22] S. Sesia, I. Toufik, and M. Baker, LTE - The UMTS Long Term Evolution, *From Theory to Practice*. John Wiley & Sons, 2011.

[23] G. Bianchi, “Performance analysis of the ieee 802.11 distributed coordination function,” *IEEE J. Sel. Areas Commun*, vol. 18, no. 3, pp. 535–547, Mar. 2000.

[24] IEEE 802.11ac, “Part 11: Wireless LAN Medium Access Control (MAC) and Physical Layer (PHY) Specifications: Enhancements for very high throughput for operation in bands below 6 GHz,” IEEE Std., Dec. 2013.

[25] A. Abdelfattah and N. Malouch, “Modeling and performance analysis of wi-fi networks coexisting with lte-u,” in *Proc. IEEE INFOCOM*, 2017, pp. 1–9.

[26] J. C. S. Arenas, T. Dudda, and L. Falconetti, “Ultra-low latency in next generation lte radio access,” in *Proc. VDE SCC*, 2017, pp. 1–6.

[27] J. Yi, W. Sun, S. Park, and S. Choi, “Performance analysis of lte-laa network,” *IEEE Commun. Lett.*, vol. 22, no. 6, pp. 1236–1239, 2017.

[28] The network simulator-3. [Online]. Available: https://www.nsnam.org/

[29] V. Sathya, S. M. Kala, M. I. Rochman, M. Ghosh, and S. Roy, “Standardization advances for cellular and wi-fi coexistence in the unlicensed 5 and 6 ghz bands,” *GetMobile: Mobile Computing and Communications*, vol. 24, no. 1, pp. 5–15, 2020.

[30] G. Gür, “Expansive networks: Exploiting spectrum sharing for capacity boost and 6g vision,” *IEEE J. Commun. Netw.*, vol. 22, no. 6, pp. 444–454, 2020.

[31] T. Tao, F. Han, and Y. Liu, “Enhanced lbt algorithm for lte-laa in unlicensed band,” in *Proc. IEEE PIMRC*, 2015, pp. 1907–1911.

[32] A. V. Kini, L. Canonne-Velasquez, M. Hosseinian, M. Rudolf, and J. Stern-Berkowitz, “Wi-fi-laa coexistence: Design and evaluation of listen before talk for laa,” *Proc. IEEE CISS*, pp. 157–162, 2016.

[33] Z. Ali, L. Giupponi, J. Mangues-Bafalluy, and B. Bojovic, “Machine learning based scheme for contention window size adaptation in lte-laa,” in *Proc. IEEE PIMRC*, 2017, pp. 1–7.

[34] N. Bitar, M. O. A. Kalaa, S. J. Seidman, and H. H. Refai, “On the coexistence of lte-laa in the unlicensed band: Modeling and performance analysis,” *IEEE Access*, vol. 6, pp. 52 668–52 681, 2018.

[35] Y. Song, W. Ki, and Y. Han, “Coexistence of wi-fi and cellular with listen-before-talk in unlicensed spectrum,” *IEEE Commun. Lett.*, vol. 20, no. 1, pp. 161–164, 2016.

[36] C. Cheng, R. Ratasuk, and A. Ghosh, "Downlink performance analysis of lte and wifi coexistence in unlicensed bands with a simple listen-before-talk scheme," in *IEEE 81st Veh. Technol. Conf. (VTC Spring)*, 2015, pp. 1–5.

[37] M. Mehrnoush, S. Roy, V. Sathya, and M. Ghosh, "On the fairness of wi-fi and lte-laa coexistence," *IEEE Trans. Cognitive Commun. Netw.*, vol. 4, no. 4, pp. 735–748, 2018.

[38] K. Yoon, W. Sun, and S. Choi, "Coala: Collision-aware link adaptation for lte in unlicensed band," in *Proc. IEEE SECON*, 2018, pp. 1–9.

[39] P. Kutsevol, V. Loginov, E. Khorov, and A. Lyakhov, "New collision detection method for fair lte-laa and wi-fi coexistence," in *Proc. IEEE PIMRC*, 2019, pp. 1–6.

[40] V. Loginov, E. Khorov, A. Lyakhov, and I. Akyildiz, "Cr-lbt: Listen-before-talk with collision resolution for 5g nr-u networks," *IEEE Transactions on Mobile Computing*, 2021.

[41] M. Aslam, X. Jiao, W. Liu, and I. Moerman, "An approach to achieve zero turnaround time in tdd operation on sdr front-end," *IEEE Access*, vol. 6, pp. 75 461–75 470, 2018.

[42] J. Kim, J. Yi, and S. Bahk, "Uplink channel access enhancement for cellular communication in unlicensed spectrum," *IEEE Access*, vol. 8, pp. 216 386–216 397, 2020.

초 록

3세대 파트너십 프로젝트는 기존 LTE의 부족한 대역폭 문제에 대한 대안으로 넓은 비면허 대역을 사용하는 라이선스 지원 접속을 표준화하고 있다. 비면허 대역에서 3GPP 셀룰러 통신은 LBT 동작을 완료한 후에만 전송을 허용한다. 다운링크의 경우 LBT 작업을 통해 셀룰러 트래픽이 와이파이 트래픽과 잘 공존할 수 있습니다. 그러나, 셀룰러 업링크 전송은 LBT 성공 후 기지국에 의해 특별히 결정된 시간에만 시도되며, 사용자 장비는 와이파이의 간섭으로 인해 전송 실패와 전송 지연을 겪을 확률이 높다. 따라서 셀룰러 업링크 트래픽이 와이파이 트래픽과 잘 공존하지 못한다. 라이선스 지원 접속 기술은 또한 채널 액세스 메커니즘이 와이파이의 채널 액세스 메커니즘과 유사하기 때문에 동시 전송으로 충돌 문제를 겪고 있다. 와이파이는 RTS/CTS 메커니즘을 통해 충돌 문제를 해결한다. 그러나 현재 라이선스 지원 접속 기술은 충돌 문제를 해결할 방법이 존재하지 않는다. 따라서 라이선스 지원 접속 기술은 경합 노드 수가 증가함에 따라 충돌로 인해 심각한 성능 저하를 겪는다. 본 논문에서는 비면허 대역에서 셀룰러 통신에 대한 다음과 같은 두 가지 개선을 고려한다. (i) 업링크 성능 저하를 해결하기 위한 업링크 채널 액세스 향상 및 (ii) 효율적인 채널 활용을 위한 충돌 최소화. 첫째, 업링크 채널 액세스를 위한 셀룰러와 와이파이 사이의 불공정성 문제를 수학적으로 분석한다. 비면허 대역에서의 공존 문제를 해결하기 위해, 우리는 단말이 최소 길이의 업링크 예약 신호를 사용하고 기지국이 단말의 업링크 전송에 대한 최적의 타이밍을 결정할 수 있는 UpChance라는 표준을 만족하는 상향 링크 채널 접근 방식을 제안한다. ns-3 시뮬레이션을 통해 UpChance가 공정성과 랜덤 액세스 완료 시간을 각각 최대 88%, 99% 향상시키는

것을 검증한다. 둘째, 우리는 전방 예약신호와 후방 예약신호로 구성된 분할 예약 신호를 사용하고 경합 창 크기를 추가적으로 제어하는 *R-SplitC*라는 새로운 충돌 최소화 체계를 제안한다. 새로운 분할 예약 신호는 라이선스 지원 접속 기술의 전송간의 충돌을 최소화하는 데 도움을 주며, 경합 창 크기 제어는 와이파이와 같은 다른 통신 기술의 성능을 보호한다. 우리는 우리 체계의 성능을 수학적으로 분석하고 평가하여 *R-SplitC*가 와이파이 성능을 저하시키지 않고 기존의 예약 신호 체계에 비해 네트워크 처리량을 최대 100.6% 향상시키는 것을 확인한다. 요약하면, 우리는 비면허 대역에서 셀룰러 통신을 위한 업링크 채널 액세스 향상 기법 및 충돌 최소화 기법을 제안한다. 본 연구를 통해, 우리는 최첨단 기술에 비해 처리량 및 공정성과 같은 네트워크 성능의 향상을 달성한다.

주요어: 상향 링크, 비면허 대역, 충돌, 예약 신호

학번: 2014-21603

감사의 글

대학원에 입학하고 신입생으로 연구실 생활을 하던 것이 엊그제 같은데 어느덧 7년 반이 지나 졸업을 하게 되었습니다. 대학원 과정에서 도움을 주신 분들에게 이 글을 통해 감사의 말씀을 드리고자 합니다.

먼저 현 지도교수님이신 박세웅 교수님께 감사드립니다. NETLAB에 신입생으로 들어온 것이 아니라 다른 연구실에서 넘어온 학생 임에도 불구하고 기존의 네트워크 연구실 학생들과 동등하게 자애롭게 대해주시고 연구적으로 많이 이끌어주신 점에 대해서 감사드립니다. 2년이라는 길지 않은 시간이었지만 연구와 삶을 살아가는 태도 등 많은 것을 배울 수 있었습니다.

제 첫 지도교수님이신 최성현 교수님께 감사드립니다. 학부때 데이터 통신망의 기초 수업의 명강의를 들으면서 연구실 진학을 꿈꿨고 대학원 진학 후 5년 반이라는 긴 시간 동안 지도를 받으면서 연구의 기본부터 삶을 살아가는 태도까지 많은 것을 보고 또 많이 혼나면서 배우고 성장할 수 있었습니다. 아쉽게 박사과정의 끝까지 지도를 받지는 못했지만 현실에 안주하지 않고 더 큰 꿈을 찾으시는 모습을 보며 많은 감명을 받았습니다.

토요일 오전의 논문 세미나를 함께 하셨던 이병기 교수님께 감사드립니다. 대학원에 들어와서 많은 논문들을 보고 듣고 발표하면서 논문을 읽는 법과 요약해서 발표하는 법들을 기초부터 배울 수 있었습니다.

박사 학위논문 심사를 맡아주신 김성철 교수님, 최완 교수님, 이경한 교수님, 주창희 교수님께 감사드립니다. 심사를 통해서 많은 조언들을 해주신 덕분에 학위 논문의 완성도를 높일 수 있었습니다.

연구실 생활을 같이한 선후배님들에게도 감사합니다. 오랜 시간을 같은 공간

에서 생활하면서 많은 도움을 받았습니다. 이전 연구실인 MWNL과 현 연구실인 NETLAB에서 모두 좋은 사람들만 만난 것 같습니다. 앞으로 같은 곳에서 일하게 된다면 받은 것 보다 더 많은 도움을 주고 싶습니다.

언제나 지지해주고 응원해주신 아버지와 어머니께 감사드립니다. 오랜 시간 묵묵히 응원해 주셔서 여기까지 올 수 있었습니다. 기숙사에서 주로 지내면서 많이 찾아 뵙지 못했는데 앞으로 더 자주 뵈면서 효도하겠습니다. 자주 만나지 못하지만 항상 즐겁게 대해주는 누나들, 그리고 매형들께도 감사드립니다.

마지막으로 언제나 응원해준 사랑하는 주영이에게 감사드립니다. 학부 때부터 항상 저의 선택을 존중해주고 오랜 대학원생 기간에도 항상 응원해주고 격려해주고 위로해줘서 감사합니다.

다시 한 번 모든 분들께 감사드리며 이 논문을 바칩니다.

2021년 8월

김지훈 올림